

See discussions, stats, and author profiles for this publication at: <https://www.researchgate.net/publication/5646956>

Energetics and Mechanism of the Decomposition of Trifluoromethanol

ARTICLE in THE JOURNAL OF PHYSICAL CHEMISTRY A · MARCH 2008

Impact Factor: 2.69 · DOI: 10.1021/jp709796n · Source: PubMed

CITATIONS

12

READS

18

6 AUTHORS, INCLUDING:



Vu Thi Ngan

Quy Nhon University

32 PUBLICATIONS 559 CITATIONS

SEE PROFILE



Ralf Haiges

University of Southern California

141 PUBLICATIONS 1,153 CITATIONS

SEE PROFILE



Karl O Christe

University of Southern California

530 PUBLICATIONS 6,934 CITATIONS

SEE PROFILE



David A Dixon

University of Alabama

767 PUBLICATIONS 22,217 CITATIONS

SEE PROFILE

Energetics and Mechanism of the Decomposition of Trifluoromethanol

Minh Tho Nguyen,^{†,‡} Myrna H. Matus,[†] Vu Thi Ngan,[‡] Ralf Haiges,[§] Karl O. Christe,[§] and David A. Dixon^{*,†}

Department of Chemistry, The University of Alabama, Shelby Hall, Tuscaloosa, Alabama 35487-0336,
Department of Chemistry, University of Leuven, B-3001 Leuven, Belgium, and Loker Research Institute and
Department of Chemistry, University of Southern California, Los Angeles, California 90089-1661

Received: October 7, 2007; In Final Form: October 16, 2007

The thermal instability of α -fluoroalcohols is generally attributed to a unimolecular 1,2-elimination of HF, but the barrier to intramolecular HF elimination from CF_3OH is predicted to be 45.1 ± 2 kcal/mol. The thermochemical parameters of trifluoromethanol were calculated using coupled-cluster theory (CCSD(T)) extrapolated to the complete basis set limit. High barriers of 42.9, 43.1, and 45.0 kcal/mol were predicted for the unimolecular decompositions of CH_2FOH , CHF_2OH , and CF_3OH , respectively. These barriers are lowered substantially if cyclic H-bonded dimers of CF_3OH with complexation energies of ~ 5 kcal/mol are involved. A six-membered ring dimer has an energy barrier of 28.7 kcal/mol and an eight-membered dimer has an energy barrier of 32.9 kcal/mol. Complexes of CF_3OH with HF lead to strong H-bonded dimers, trimers and tetramers with complexation energies of ~ 6 , 11, and 16 kcal/mol, respectively. The dimer, $\text{CH}_3\text{OH}:\text{HF}$, and the trimers, $\text{CF}_3\text{OH}:\text{2HF}$ and $(\text{CH}_3\text{OH})_2:\text{HF}$, have decomposition energy barriers of 26.7, 20.3, and 22.8 kcal/mol, respectively. The tetramer $(\text{CH}_3\text{OH}:\text{HF})_2$ gives rise to elimination of two HF molecules with a barrier of 32.5 kcal/mol. Either CF_3OH or HF can act as catalysts for HF-elimination via an H-transfer relay. Because HF is one of the decomposition products, the decomposition reactions become autocatalytic. If the energies due to complexation for the $\text{CF}_3\text{OH}-\text{HF}$ adducts are not dissipated, the effective barriers to HF elimination are lowered from ~ 20 to ~ 9 kcal/mol, which reconciles the computational results with the experimentally observed stabilities.

Introduction

Trifluoromethanol (CF_3OH), the simplest perfluorinated primary alcohol, was first synthesized from CF_3OCl by reaction with HCl by Seppelt in 1977.^{1,2} However, until the recent discovery of a more convenient synthesis by Christe and co-workers,³ it has not been readily accessible for studying its reaction chemistry because it was difficult to prepare, is unstable, and undergoes facile HF elimination at room temperature. Christe's approach, in fact, takes advantage of this process as COF_2 in anhydrous HF is in equilibrium with CF_3OH . Furthermore, CF_3OH has been proposed as an intermediate in the atmospheric degradation of hydrofluorocarbons (HFC), which are replacements for the chlorofluorocarbons. The trifluoromethoxy $\text{CF}_3\text{O}^\bullet$ radical can be formed in the atmospheric oxidation of HFCs.⁴ This radical has been proposed to abstract H from organic compounds in the atmosphere leading to the formation of CF_3OH .⁵ Thus, an important question is as to whether CF_3OH could act as a temporary reservoir for $\text{CF}_3\text{O}^\bullet$ in the atmosphere.⁶ In addition, it has been found that chemically activated CF_3OH produced by the reaction of $\text{O}(^1\text{D})$ with HFC's is unstable toward dissociation giving CF_2O and hydrogen fluoride.^{7–10}

Francisco¹¹ used quantum chemical approaches to study the primary and secondary dissociation pathways of CF_3OH and showed that the 1,2-elimination of HF constitutes the thermo-

dynamically and kinetically most favored route. This unimolecular route has a substantial potential energy barrier of 45.1 ± 2 kcal/mol (QCISD(T)/6-311G(2df,2p) + ZPE corrections).¹¹ In a subsequent theoretical study at the MP4/TZ2P level, Schneider et al.¹² reported a slightly smaller energy barrier of 42 ± 3 kcal/mol. At 298 K, this barrier leads to a first-order rate constant of $\sim 10^{-17} \text{ s}^{-1}$. Such a rate is too low for this molecular process to be observed in the atmosphere but could be consistent with experimental results at elevated temperatures.¹³

Lovejoy et al.¹⁴ observed a large increase in the decomposition rate of CF_3OH in bulk water and in sulfuric acid solution. Schneider et al.¹² in their computational study showed that a water-mediated process, where the water molecule serves as a hydrogen shuttle between oxygen and fluorine within a six-member cyclic transition structure, led to a reduction in the energy barrier to about 17 kcal/mol with respect to the separated system $\text{CF}_3\text{OH} + \text{H}_2\text{O}$. The large catalytic effect of compounds such as HF and H_2O involving a cyclic transition state (TS) with concerted H-transfer has been well documented.^{15,16}

Doering et al.¹⁷ predicted on the basis of HF/6-311++G-(2d,2p) calculations that CF_3OH forms hydrogen-bonded dimers and trimers. In particular, a dimer is formed by involving the OH group of one monomer with the FCOH skeleton of the other, giving rise to a six-member cyclic complex. Although the resulting dimerization energy of ~ 3 kcal/mol is relatively small (stabilizing the dimer), the dimer constitutes a potential pre-association complex for a HF-elimination. This leads to the possibility that in a water-free medium, CF_3OH could undergo decomposition involving dimers. Although the question has been

* Corresponding author. E-mail: dadixon@bama.ua.edu.

[†] The University of Alabama.[‡] University of Leuven.[§] University of Southern California.

raised what effect complex formation could have on the removal of CF₃OH in the atmosphere,¹⁸ as far as we are aware, no studies of such processes have been reported. The fact that Christe et al.³ found an equilibrium between CF₃OH and COF₂ plus anhydrous HF, also suggests a possible active participation of the existing HF molecules in an autocatalytic process. A comparable mechanism was earlier proposed for the pyrolysis of formic acid, in which some of the water molecules produced by the initial dehydration could serve as catalysts for the decarboxylation path.¹⁹

The thermochemical parameters of CF₃OH have been the subject of some debate.^{18,20–22} Numerous experimental and theoretical results have been reported for the bond dissociation energy (BDE) and standard heat of formation.^{23–32} Available results for the BDE(CF₃O–H) range from 109 ± 2.5²³ to 120 ± 3²⁴ kcal/mol, with the most recent experimental value being = 117.5 (+1.9/–1.4)³¹ kcal/mol as compared to a B3LYP value of 118.8 ± 0.5 kcal/mol.³² (The low error estimate at the DFT level is not justified in terms of the accuracy of the method.) Results for Δ*H*_{f,298}(CF₃OH) from previous experimental and theoretical studies range from –213.5 to –220.7 kcal/mol. The two most recent experimental values for this parameter are –220.7 ± 3.2³⁰ and ≥ –217.2 ± 0.9³¹ kcal/mol. The most reliable theoretical result to date of –217.7 ± 2.0 kcal/mol was evaluated using the G2 method.³¹ Other basic thermochemical properties of CF₃OH that have determined include its proton affinity,³⁰ gas phase acidity,^{33,34} and ionization potential.³¹ Uncertainties in both the Δ*H*_f and BDE values show that the heat of formation of the CF₃O• radical is also subject to a rather large range, even though the electronic structure and spectroscopic properties of this reactive species have been well characterized.^{35–38} The adiabatic electron affinity of CF₃O• has been reported to vary over a wide range from 3.25 to 4.26 eV.^{39–42}

The aim of the present theoretical study is 2-fold. First, we reinvestigate the basic thermodynamic properties of CF₃OH and relevant derivatives by using high-accuracy electronic structure computations following an approach developed by our laboratory in conjunction with work at the Pacific Northwest National Laboratory and Washington State University.⁴³ As an example, we have theoretically determined the fundamental parameters for methanol and ethanol derivatives with accuracies of ±0.5 kcal/mol for methanol, and ±0.8 kcal/mol for ethanol,⁴⁴ in excellent agreement with the most recent experimental determinations. We have applied the same computational methodology to predict the thermochemical properties of CF₃OH. Second, we have explored the molecular pathways for HF-elimination from CF₃OH and its dimers, without and with the presence of one and two HF molecules.

Computational Methods

Electronic structure calculations were carried out by using the Gaussian 03,⁴⁵ and MOLPRO⁴⁶ suites of programs. The enthalpies of formation of CF₃OH and each of its derivatives were determined from the corresponding total atomization energies (TAE). Geometry parameters of each structure considered were fully optimized using molecular orbital theory at the second-order perturbation MP2 level with the correlation-consistent aug-cc-pVTZ basis set. The fully unrestricted formalism (UHF, UMP2) was used for open-shell system calculations done with Gaussian 03. The single-point electronic energies were calculated at the MP2/aug-cc-pVTZ geometries using the coupled-cluster CCSD(T) formalism^{47–50} in conjunction with the correlation-consistent aug-cc-pVnZ (*n* = D, T, and Q) basis

sets.⁵¹ For simplicity, the basis sets are denoted hereafter as aVnZ. Only the spherical components (5d, 7f, 9g) of the Cartesian basis functions were used. The open-shell CCSD(T) calculations for the atoms were carried out at the R/UCCSD(T) level. In this approach, a restricted open shell Hartree–Fock (ROHF) calculation was initially performed and the spin constraint was relaxed in the coupled cluster calculation.^{52–54} The CCSD(T) energies were extrapolated to the complete basis set (CBS) limit energies using the following expression:⁵⁵

$$E(x) = A_{\text{CBS}} + B \exp[-(x - 1)] + C \exp[-(x - 1)^2] \quad (1)$$

After the valence electronic energy, the largest contribution to the TAE is the zero-point energy (ZPE). Harmonic vibrational frequencies of each of the monomeric species were calculated at the equilibrium geometry using the (U)MP2/aVTZ method. We obtained an estimate of the anharmonic corrections that are largest for the O–H and C–H stretches. A scaling factor for the O–H stretches of 0.9798 was obtained by averaging the calculated MP2/aVTZ value (3829.8 cm^{–1}) with the experimental value^{56,57} (3675 cm^{–1}) and dividing by the MP2 value. For the C–H stretches, we obtained a scale factor of 0.9701 in a similar way using the experimental values^{58,59} (2844, 2962, and 2999 cm^{–1}) for CH₃OH. These scale factors were used for all of molecules, radicals, ions, and transition state structures derived from the monomeric alcohols.

To evaluate the TAE's, smaller corrections are also required. Core–valence correlation corrections (Δ*E*_{CV}) were obtained at the CCSD(T)/cc-pwCVTZ level of theory.⁶⁰ Scalar relativistic corrections (Δ*E*_{SR}), which account for changes in the relativistic contributions to the total energies of the molecule and the constituent atoms, were included at the CI-SD (configuration interaction singles and doubles) level of theory using the cc-pVTZ basis set. Δ*E*_{SR} is taken as the sum of the mass-velocity and 1-electron Darwin (MVD) terms in the Breit–Pauli Hamiltonian.⁶¹ Most calculations using available electronic structure computer codes do not correctly describe the lowest energy spin multiplet of an atomic state, as spin–orbit in the atom is usually not included. Instead, the energy is a weighted average of the available multiplets. The spin–orbit corrections are 0.085 kcal/mol for C, 0.223 kcal/mol for O, and 0.380 kcal/mol for F, all of them from the excitation energies of Moore.⁶²

The total atomization energy (Σ*D*₀ or TAE) of a compound is given by the expression

$$\Sigma D_0 = \Delta E_{\text{elec}}(\text{CBS}) + \Delta E_{\text{ZPE}} + \Delta E_{\text{CV}} + \Delta E_{\text{SR}} + \Delta E_{\text{SO}} \quad (2)$$

By combining our computed Σ*D*₀ values with the known heats of formation⁶³ at 0 K for the elements (Δ*H*_f⁰(H) = 51.63 ± 0.001 kcal/mol, Δ*H*_f⁰(C) = 169.98 ± 0.1 kcal/mol, Δ*H*_f⁰(O) = 58.99 ± 0.1 kcal/mol, and Δ*H*_f⁰(F) = 18.47 ± 0.07 kcal/mol), we can derive Δ*H*_f⁰ values at 0 K for the molecules in the gas phase. We obtain heats of formation at 298 K by following the procedures outlined by Curtiss et al.⁶⁴ All other thermochemical parameters were derived from the corresponding heats of formation.

To model the HF-elimination reactions, we first constructed the unimolecular pathways for the three fluorinated methanols CH_xF_yOH, with *x* + *y* = 3. We also considered pathways for loss of HF from the dimer (CF₃OH)₂, and in the presence of one and two HF molecules including CF₃OH + HF, CF₃OH + (HF)₂, (CF₃OH)₂ + HF, and (CF₃OH)₂ + (HF)₂.

Geometries of the relevant equilibrium and transition state structures (TS) were optimized at the MP2 level with both aVDZ and aVTZ basis sets. Harmonic vibrational frequencies for

monomers and CF₃OH–HF were calculated at the MP2/aVTZ level; frequencies of the larger dimeric systems were, however, calculated only at the MP2/aVDZ level. For this level, a scaling factor of 0.9823 for the O–H stretch was obtained as described above. Relative energies were calculated from coupled-cluster CCSD(T) energies based upon MP2/aVTZ optimized geometries and the aVnZ basis sets. For the monomeric systems, CBS energies were extrapolated as described above. For the dimers, we calculated the CCSD(T)/aVTZ and MP2/CBS energies. We estimated the CBS correction to the CCSD(T)/aVTZ values from the MP2 calculations as

$$\Delta E[\text{CCSD(T)/CBS}] = \Delta E[\text{CCSD(T)/aVTZ}] + (\Delta E[\text{MP2/CBS}] - \Delta E[\text{MP2/aVTZ}]) \quad (3)$$

The kinetics for the HF elimination was studied with conventional transition state theory (TST)^{65,66} The thermal rate constant in the thermodynamic formulation is given by⁶⁵

$$k_{\infty}(\text{TST}) = \frac{k_B T}{h} \exp \frac{\Delta S^{\ddagger}}{R} \exp \frac{-\Delta H^{\ddagger}}{RT} \quad (4)$$

and the high-pressure limit pre-exponential factor is thus given by $A = (k_B T/h) \exp(\Delta S^{\ddagger}/R)$. Note that the E_a of the Arrhenius expression from TST and ΔH^{\ddagger} are related by $E_a = \Delta H^{\ddagger} + RT$ for a unimolecular process.

We also used RRKM theory⁶⁷ to predict the rate constants using the following expression:

$$k_{\text{uni}} = \frac{\sigma}{h} \left[\frac{N^{\ddagger}(E - E_0)}{\rho(E)} \right] \quad (5)$$

where σ is the symmetry number. Evaluation of the sum (N^{\ddagger}) and density (ρ) of states was carried out using the KHIMERA program.⁶⁸ We calculated the tunneling corrections using the Skodje and Truhlar (ST)⁶⁹ equations, which include the imaginary frequency, the energy barrier, and the reaction energy. ΔH^{\ddagger} , the zero point corrected barrier height, and ΔH_R , the reaction exothermicity, both at 0 K:

$$Q_{\text{tunnel,ST}}(T) = \frac{\beta\pi/\alpha}{\sin(\beta\pi/\alpha)} - \frac{\beta}{\alpha - \beta} \exp[(\beta - \alpha)(\Delta H^{\ddagger} - \Delta H_R)] \quad (6a)$$

this expression is valid for $\alpha \geq \beta$. In the case where $\beta \geq \alpha$:

$$Q_{\text{tunnel,ST}}(T) = \frac{\beta}{\beta - \alpha} \{ \exp[(\beta - \alpha)(\Delta H^{\ddagger} - \Delta H_R)] - 1 \} \quad (6b)$$

with $\beta = 1/k_B T$ and $\alpha = 2\pi/\hbar\omega_i$ and ω_i is the imaginary frequency at the transition state; when the reaction is exoergic, ΔH_R is equal to zero.

Results and Discussion

Total energies of the molecules are given in Table S1 of the Supporting Information, vibrational modes and unscaled ZPEs are given in Table S2, and MP2/aVTZ optimized geometries of all structures considered are listed in Table S3. The components that are used to predict the total atomization energies and the TAE (ΣD_0) are given in Table 1. The predicted enthalpies of formation at both 0 and 298 K are summarized in Table 2. Thermochemical parameters are listed in Table 3 and, where possible, compared with experiment.

Thermochemical Parameters of Trifluoromethanol and Derivatives. Several experimental and theoretical investigations of the heat of formation and bond dissociation energy of CF₃OH have been reported. The available data have been analyzed by

TABLE 1: Components for Calculated Atomization Energies in kcal/mol

molecule	CBS ^a	ΔE_{ZPE}^b	ΔE_{CV}^c	ΔE_{SR}^d	ΔE_{SO}^e	$\Sigma D_0(0 \text{ K})$
CF ₃ OH (¹ A')	571.51	-18.15	1.24	-1.37	-1.448	551.78
CF ₃ O• (² A')	444.85	-10.23	1.03	-1.19	-1.448	433.00
CF ₃ O ⁺ (³ A ₁)	133.69	-9.62	2.12	-0.92	-1.448	123.81
CF ₃ O ⁻ (¹ A ₁)	549.16	-9.68	1.18	-1.36	-1.448	537.85
CF ₃ OH ⁺ (² A'')	268.68	-16.30	0.85	-1.14	-1.448	250.64
CF ₃ OH ₂ ⁺ (¹ A')	411.60	-25.47	1.17	-1.36	-1.448	384.50
HF–CF ₂ OH ⁺ (¹ A)	416.67	-23.72	1.36	-1.32	-1.448	391.53
CF ₂ OH ⁺ –FH (¹ A')	422.15	-23.63	1.39	-1.34	-1.448	397.12
CF ₃ (² A ₁)	345.49	-7.71	0.89	-0.94	-1.225	336.50
CF ₂ O (¹ A ₁)	419.57	-8.80	1.24	-0.97	-1.068	409.98
CF ₂ O ⁺ (² B ₂)	119.24	-8.88	0.87	-0.77	-1.068	109.39
CF ₃ OH-ts (¹ A')	523.10	-14.74	2.09	-1.29	-1.448	507.71
CHF ₂ OH (¹ A)	552.28	-23.09	1.22	-1.07	-1.068	528.27
CHF ₂ OH-ts (¹ A)	505.48	-19.39	2.17	-0.99	-1.068	486.20
CH ₂ FOH (¹ A')	529.62	-28.24	2.19	-0.80	-0.688	502.08
CH ₂ FOH-ts (¹ A')	480.26	-21.75	1.07	-0.71	-0.688	458.18

^a From CCSD(T)/CBS energies extrapolated using eq 1, with aVnZ basis sets, where $n = \text{D, T and Q}$, based on at the MP2/aVTZ optimized geometries, unless otherwise noted. Total energies are given in Table S1 (Supporting Information). ^b Calculated zero-point energies are reported in Table S2 (Supporting Information). Scaling factors of 0.9798 and 0.9701 were applied on the vibrational modes corresponding to the O–H and C–H stretchings, respectively. ^c Core/valence corrections were obtained with the cc-pwCVTZ basis sets. ^d The scalar relativistic correction (MVD) is from CISD/aVTZ calculations. ^e Atomic spin-orbit corrections from ref 62.

TABLE 2: CCSD(T)/CBS Heats of Formation at 0 and 298 K (kcal/mol) Compared to Experiment and MP2/aVTZ Entropies (cal/(mol K))

molecule	$\Delta H_f(0 \text{ K})$ this work	$\Delta H_f(298 \text{ K})$ this work	$\Delta H_f(298 \text{ K})$ exptl	S
CF ₃ OH (¹ A')	-215.8	-217.8	-217.2 ± 0.9 ^a	69.24
CF ₃ O• (² A')	-148.6	-149.8	-151.8	69.75
CF ₃ O ⁺ (³ A ₁)	160.6	160.0		73.53
CF ₃ O ⁻ (¹ A ₁)	-253.5	-254.7		65.95
CF ₃ OH ⁺ (² A'')	85.4	83.8		74.03
CF ₃ OH ₂ ⁺ (¹ A')	3.1	0.4	-6.1 ± 2.4	71.57
HF–CF ₂ OH ⁺ (¹ A)	-3.9	-5.6		80.12
CF ₂ OH ⁺ –FH (¹ A')	-9.5	-11.4	-19.6	79.33
CF ₃ (² A ₁)	-111.1	-111.8		63.18
CF ₂ O (¹ A ₁)	-144.1	-144.8	-149.1	61.87
CF ₂ O ⁺ (² B ₂)	156.5	155.8	151.2	63.41
CF ₂ OH ⁺ (¹ A')	73.7	72.0		63.73
HF–CFO ⁺ (¹ A')	94.5	94.2		73.26
CF ₃ OH-ts (¹ A')	-171.7	-173.9		68.95
CHF ₂ OH (¹ A)	-159.1	-161.5		65.38
CHF ₂ OH-ts (¹ A)	-117.0	-119.5		65.69
CH ₂ FOH (¹ A')	-99.8	-102.4		61.37
CH ₂ FOH-ts (¹ A')	-55.8	-58.5		61.11

^a -215.3 kcal/mol at 0 K.

different authors.^{31,32} In particular, Table 1 of ref 31 provides a detailed chronological order. Batt and Walsh²³ used a group additivity approach and obtained $\Delta H_{f,298}(\text{CF}_3\text{OH}) = -213.5 \pm 1.5$ kcal/mol. These authors also studied experimentally the kinetics of the pyrolysis of the peroxides and derived $\Delta H_{f,298}(\text{CF}_3\text{O}^\bullet) = -157 \pm 1.5$ kcal/mol and a corresponding BDE-(CF₃O–H) = 108.9 kcal/mol. Using isodesmic reactions with Hartree–Fock energies, Sana et al.²⁵ obtained a value of $\Delta H_{f,298}(\text{CF}_3\text{OH}) = -217.4$ kcal/mol. Wallington et al.^{12,24} carried out kinetic experiments on the reaction of CF₃O• with water, and from the heat of reaction (CF₃O + H₂O → CF₃OH + OH) obtained at the MP2/6-311+G(d,p) level, they derived BDE(CF₃O–H) = 120 ± 3 kcal/mol, clearly larger than that derived by Batt and Walsh. The Ford group subsequently refined their calculations by carrying out geometry optimizations at the second-order perturbation theory MP2/6-31(d,p) level and single-point electronic energies using the full fourth-order perturbation level MP4SDTQ/6-311+G(d,p), and they obtained

TABLE 3: Calculated Thermochemical Parameters of Trifluoromethanol and Its Derivatives Compared to Experiment^a

parameter	calculated	experiment (ref)
IE _a (CF ₃ OH), eV	13.06	≤13.08 ± 0.05 (31)
PA _O (CF ₃ OH), kcal/mol	147.5	151.1 ± 1.7 (30)
PA _F (CF ₃ OH), kcal/mol	159.3	164.6 (30)
ΔH _{acid} (CF ₃ O–H), kcal/mol	328.8	329.8 ± 2 (33)
BDE(CF ₃ O–H), kcal/mol	118.8	117.5 (31)
BDE(CF ₃ –OH), kcal/mol	113.5	≤115.2 ± 0.3 (31)
EA(CF ₃ O), eV	4.55	4.70 ± 0.13 (33)
IE _a (CF ₃ O), eV	13.41	
BDE(CF ₃ –O), kcal/mol	96.5	
BDE(CF ₂ O–F), kcal/mol	23.0	27 ± 2 (32)
PA(CF ₃ O [•]), kcal/mol	132.1	
PA _O (CF ₂ O), kcal/mol	149.0	≤132.4 + 1.7/–1.2 (31) 159.9 (72)
PA _F (CF ₂ O), kcal/mol	126.7	
IE _a (CF ₂ O), eV	13.03	13.024 (31)
FA(CF ₂ O) kcal/mol	50.5	49.9 (75)

^a ΔH_f(H⁺) = 365.2 kcal/mol at 0 K and ΔH_f⁰(H⁺) = 365.7 kcal/mol at 298 K. ΔH_f(F[•]) = –59.96 (0 K) and –59.46 (298 K) kcal/mol. Reference 63.

a value of ΔH_{f,298}(CF₃OH) = –217.7 ± 2.0 and 119 kcal/mol for the BDE.²⁷ Benson²⁰ disagreed with the predicted values and suggested a value of ΔH_{f,298}(CF₃OH) = –215 ± 1 and 109 ± 2.5 kcal/mol for the BDE. The latter BDE result was, however, not supported by other molecular orbital theory calculations. Dixon and Fernandez²⁶ reported a BDE of 119.4 ± 1.5 kcal/mol at the MP2 level with a polarized double-ζ basis set using isodesmic reactions, and Bock et al.²⁸ reported values up to 121.9 kcal/mol. Using the composite G2 method, Montgomery et al.²⁹ obtained ΔH_{f,298}(CF₃OH) = –217.7 ± 2.0 kcal/mol. Experimentally, Chyall and Squires³⁰ determined the proton affinity of CF₃OH using mass spectrometric techniques, and derived ΔH_{f,298}(CF₃OH) = –220.7 ± 3.2 kcal/mol. Asher et al.³¹ carried out photoionization experiments on CF₃OH and related species and derived ΔH_{f,298}(CF₃OH) ≥ –217.2 ± 0.9 kcal/mol. The corresponding lower and upper limits of these two experimental values overlap. Using isodesmic reactions with DFT/B3LYP energies, Reints et al.³² obtained BDE(CF₃O–H) = 118.8 ± 0.5 kcal/mol. We note that in the recent NASA compilation,⁷⁰ a value of ΔH_{f,298}(CF₃OH) = –218 ± 2 kcal/mol was selected.

Table 2 lists the heats of formation evaluated from CCSD(T)/CBS calculations including all corrections. On the basis of our results recently obtained for methanol and derivatives using the same methodology,⁴⁴ we would assign an error of ±1.0 kcal/mol on the CBS-based parameters for CF₃OH. We calculate ΔH_f⁰(CF₃OH) = –217.8 ± 1.0 kcal/mol at 298 K (Table 2). Our value for ΔH_f⁰(CF₃OH) agrees with most previous theoretical results, in particular with the G2 result.²⁹ It is also close to the lower limit from the photoionization experiment³¹ and almost coincides with the NASA tabulated value.⁷⁰ The experimental heat of formation of –220.7 ± 3.2 kcal/mol³⁰ from the proton affinity measurements is too negative, but the lower range of the error bar is in agreement with the calculated values.

The HOMO of CF₃OH is of a'' symmetry (C_s point group) with bonding overlap between C and O and antibonding overlap between C and F. Removal of one electron from this molecule to form the CF₃OH^{•+} radical cation leads to a ²A'' ground state. In contrast to the methanol radical cation, whose equilibrium structure corresponds to an eclipsed conformation (HOCH dihedral angle being zero),⁴⁴ CF₃OH^{•+} maintains the staggered conformation of the neutral in its ground state (OHCF dihedral angle = 180°). The eclipsed conformer (*cis*-HOCF arrangement)

corresponds to a transition state for internal rotation. The main structural change upon ionization is the substantial lengthening of the C–O distance, from 1.347 Å in the neutral to 1.650 Å in the cation. The C–F distances also change but to a lesser extent, from 1.32 to 1.34 Å in the neutral to 1.26 to 1.27 Å in the cation. The presence of F atoms induces a separation of the charge and radical centers; the CF₃OH^{•+} radical cation can in fact be regarded as a strong complex between CF₃⁺ and OH[•]. From the calculated value for ΔH_f⁰(CF₃OH^{•+}) (Table 2) we predict an adiabatic ionization energy at 0K, IE_a(CF₃OH) = 13.06 eV (Table 3), in excellent agreement with the experimental value of 13.08 ± 0.05 eV from a photoionization study.³¹

CF₃OH can be protonated at oxygen or fluorine. Protonation in HF/SbF₅ results exclusively in protonation on oxygen.³ The O-protonated form, CF₃OH₂⁺, was also generated by Chyall and Squires³⁰ in their flowing afterglow experiments by the reaction of CF₃I⁺ with water. Using the enthalpy of the proton exchange reaction of this cation with CO, these authors determined a heat of formation ΔH_f⁰(CF₃OH₂⁺) = –6.1 ± 2.4 at 298 K and an oxygen proton affinity of PA_O(CF₃OH) = 151.1 ± 1.7 kcal/mol. We predict ΔH_f⁰(CF₃OH₂⁺) = 0.4 ± 0.8 kcal/mol at 298 K (Table 2) and a corresponding PA_O(CF₃OH) = 147.5 kcal/mol at 298 K (Table 3). The difference of 3.6 kcal/mol between our result and that of Chyall and Squires for the proton affinity is consistent with the difference in the two heats of formation of CF₃OH discussed above and we note that the experimental error bar is ±3.2 kcal/mol.

It has been observed that, in the gas phase, F-protonation of CF₃OH is favored over O-protonation.^{30,71} Our calculations are in agreement with this observation. Protonation at fluorine breaks a C–F bond, resulting in two low-energy complexes between HF and CF₂OH⁺ as found previously.³⁰ In the first complex HF–CF₂OH⁺, the F atom of HF interacts with the π(C=O) electrons. The second complex CF₂OH⁺–FH involves an O–H...F hydrogen bond with a planar structure and is 6.0 kcal/mol lower in energy than the first complex. For the most stable complex, ΔH_f⁰(CF₂OH⁺–FH) = –11.4 ± 1.0 kcal/mol at 298 K. This complex is 11.8 kcal/mol more stable than the O-protonated form giving PA_F(CF₃OH) = 159.3 kcal/mol (value at 298 K, Table 3).

Relative to the separated cation CF₂OH⁺, the OH stretching frequency in HF–CF₂OH⁺ is blue-shifted by 26 cm^{–1}, whereas that in CF₂OH⁺–FH is red-shifted by 795 cm^{–1} (from 3595 to 2800 cm^{–1}). The large frequency shift is consistent with the lengthening of the corresponding O–H bond distance in these strong hydrogen-bonded complexes by 0.043 Å. The complexation energy between HF and CF₂OH⁺ giving CF₂OH⁺–FH is calculated to be 18.1 kcal/mol, in qualitative agreement with the experimental value of 14.4 ± 1.7 kcal/mol obtained by Chyall and Squires³⁰ from a collision induced dissociation experiment. They estimated a substantially more negative heat of formation ΔH_f⁰(CF₂OH⁺–FH) = –19.6 kcal/mol, which is 13.5 kcal/mol lower than their measured heat of formation of CF₃OH₂⁺. This value was not based on a direct determination of the PA at F, but from a thermochemical cycle using an experimental value of 14.4 ± 1.7 kcal/mol for the binding energy CF₂OH⁺–FH → HF + CF₂OH⁺, together with a value for PA(CF₂O) = 160.5 kcal/mol and a heat of formation of CF₂O of –145.3 kcal/mol. The PA was based on the value of 159.9 kcal/mol obtained earlier by McMahon and co-workers⁷² from ICR proton-transfer equilibrium measurements. In a photoionization study, Asher et al.³¹ determined a much smaller value for the lower limit PA(CF₂O) ≥ 132.4 (+1.7/–1.2) kcal/mol. We note that the proton affinity of carbonyl difluoride has

not been well-established yet so we have calculated it using our approach. The calculated proton affinity at O is 149.0 kcal/mol at 298 K. This value lies between the two sets of experimental values. Because it is so different from the ion-bracketing value, we extensively searched the potential energy surface and did not find a lower energy structure for the cation. The proton affinity at F leads to the formation of a complex between HF and FCO^+ with a much lower proton affinity of 126.7 kcal/mol. These results show that new measurements of the proton affinity of CF_2O are required as our value is not expected to be in error by more than ± 1 kcal/mol.

The $\text{CF}_3\text{O}^\bullet$ radical has been the subject of a number of spectroscopic and theoretical studies.^{35,36,37,38,73} $\text{CF}_3\text{O}^\bullet$ has a $^2A'$ ground state in its C_s equilibrium geometry due to a Jahn–Teller distortion from the 2E (C_{3v}) state. The distortion results in a closing of an OCF bond angle (from 109.7 to 106.0°) and an opening of the two others OCF angles (to 111.8°). Opening one OCF bond angle (to 114.1°) and closing two others (to 108.2°) lead to a $^2A''$ structure, which has an imaginary frequency. The interplay between a small Jahn–Teller distortion and spin–orbit coupling, giving rise to interesting spin–vibronic interactions, has been analyzed in detail by Marenich and Boggs.⁷³ Due to the differences in the reported results for both the ΔH_f^0 and BDE of CF_3OH , the heat of formation of $\text{CF}_3\text{O}^\bullet$ ranges from -149 to -157 kcal/mol.^{20,32} Our CBS calculations predict $\Delta H_f^0(\text{CF}_3\text{O}^\bullet) = -149.8 \pm 0.5$ kcal/mol at 298 K (Table 2). Our value at 298 K differs significantly from the original estimate of -157 kcal/mol²⁰ but is closer to the more recent estimates of 149.2 ± 2 by Schneider and Wallington²⁷ (the NASA compilation value⁷⁰) and -150.5 kcal/mol by Reints et al.³² From our calculated heats of formation, we obtain BDE- $(\text{CF}_3\text{O}-\text{H}) = 118.8 \pm 1.0$ kcal/mol at 0 K, comparable to previous theoretical estimates. The combination of the results for $\text{CF}_3\text{O}^\bullet$ and $\text{CF}_3\text{OH}^{++}$ allows the oxygen proton affinity to be predicted as $\text{PA}_\text{O}(\text{CF}_3\text{O}^\bullet) = 132.1 \pm 0.5$ kcal/mol. Thus the radical oxygen site is ~ 15 kcal/mol less basic than that in the neutral alcohol.

Ionization of $\text{CF}_3\text{O}^\bullet$ leads to the CF_3O^+ cation, which has a triplet ground state (3A_1 C_{3v}). Similar to the $\text{CF}_3\text{OH}/\text{CF}_3\text{OH}^{++}$ pair, the C–O bond in the cation is essentially broken (2.24 Å) and the best description of the cation is a complex between CF_3^+ and a ground state O (3P). No stable singlet was located, consistent with the fact that the singlet state of the atom is 45.3 kcal/mol above the ground state.⁶² We predict an ionization energy $\text{IE}_\text{a}(\text{CF}_3\text{O}^\bullet) = 13.41$ eV, an increase of 0.35 eV with respect to the $\text{IE}_\text{a}(\text{CF}_3\text{OH})$.

Attachment of an electron to $\text{CF}_3\text{O}^\bullet$ generates the closed shell CF_3O^- anion with C_{3v} symmetry (1A_1). The anion C–O distance is significantly shorter (1.220 Å) than in the radical (1.368 Å), whereas the C–F distances are stretched (1.426 Å in the anion relative to 1.328 Å in the radical). These compare reasonably well with the distances determined for CF_3O^- in a crystal structure, $r(\text{CO}) = 1.227$ Å, $r(\text{CF}) = 1.390$ – 1.397 Å.⁷⁴ Our calculated heats of formation at 0 K (Table 3) give the electron affinity $\text{EA}(\text{CF}_3\text{O}^\bullet) = 4.55$ eV (104.9 kcal/mol). Huey et al.³³ established a limit of ≥ 89.5 kcal/mol on the latter quantity. From other thermochemical parameters, these authors estimated a value of $\text{EA}(\text{CF}_3\text{O}^\bullet) = 108.5 \pm 3.0$ kcal/mol (4.70 ± 0.13 eV). Their lower bound coincides with our predicted result. Recent DFT calculations⁴² predicted $\text{EA}(\text{CF}_3\text{O}^\bullet) = 4.1$ eV, which appears to be too low. In comparison with the electron affinity of the methoxy radical, $\text{EA}(\text{CH}_3\text{O}^\bullet) = 1.58$ eV⁴⁴ the fluorine ligands markedly increase the ability to accommodate an additional electron. The structure of this simplest perfluorinated

alkoxide anion has been explained by strong negative fluorine hyperconjugation.⁷⁴ The high stability of CF_3O^- is due in part to the extra resonance structure available to delocalize the negative charge. The fluoride affinity of CF_2O ($-\Delta H$ for the reaction of $\text{CF}_2\text{O} + \text{F}^- \rightarrow \text{CF}_3\text{O}^-$) is predicted to be 50.5 kcal/mol at 298 K. This value is in excellent agreement with a previous estimate of 49.9 kcal/mol at 298 K based on a combination of experimental and computational values.^{75,76}

There have been some experimental determinations of the gas phase acidity of CF_3OH (see ref 77 for a list of references). In the latest experiment, Huey et al.³³ used an ion–molecule reaction bracketing technique and obtained $\Delta H_\text{acid}(\text{CF}_3\text{OH}) = 329.8 \pm 2.0$ kcal/mol. Our calculated value of 328.8 kcal/mol at 298 K (Table 3) is in good agreement with this value and also with earlier theoretical results: 328.3 kcal/mol (G2),³⁴ 329.2 kcal/mol (G2MP2),³⁴ and 328.9 kcal/mol (B3LYP/6-311++G-(3df,3pd)).⁷⁸

We also re-evaluated the thermochemical parameters for CF_2O as there have been some issues with these values.^{11,27,40,79,80} The heat of formation of CF_2O is predicted to be -144.1 kcal/mol at 0 K. We had previously obtained a value of -145.2 ± 0.8 kcal/mol at the CCSD(T)/CBS level without any additional corrections except the ZPE. The difference between our current value and the older value is predominantly due to the neglect of spin–orbit in the atoms as the core–valence and relativistic corrections approximately cancel. Our calculated ionization energy $\text{IE}_\text{a}(\text{CF}_2\text{O}) = 13.04$ eV is in excellent agreement with the photoionization result of 13.024 ± 0.004 eV.⁷⁹

Unimolecular HF-Elimination from Fluorinated Methanols. Francisco¹¹ explored the potential energy surface containing the primary and secondary dissociation pathways of CF_3OH and found that the 1,2-elimination of HF is thermodynamically and kinetically the most favored route. All other processes involving HF elimination from secondary species require energies in excess of ~ 50 kcal/mol above this route. Therefore we considered only the unimolecular 1,2-HF loss pathway. For comparison, the transition state structures for unimolecular HF-eliminations from the lower homologues, mono- and difluoromethanol, were also located. The total atomization energies and heats of formation of CH_2FOH and CHF_2OH and their respective TS's CH_2FOH -ts and CHF_2OH -ts were calculated using the same approach described above and given in Tables 1 and 2.

From the heats of formation and the entropy values in Table 2, we can calculate the thermodynamics for the HF elimination from the monomer (in kcal/mol),



The reaction has a positive $\Delta H = 7.7$ kcal/mol but a negative free energy $\Delta G = -2.5$ kcal/mol at 298 K and the production of the two free particles is the driving force in the reaction.

The heat of formation of monofluoromethanol is predicted to be $\Delta H_f^0(\text{CH}_2\text{FOH}) = -99.8$ and -102.4 kcal/mol at 0 and 298 K, respectively. For difluoromethanol, we obtain $\Delta H_f^0(\text{CHF}_2\text{OH}) = -159.1$ and -161.5 kcal/mol at 0 and 298 K. Our estimated error limit is ± 1.0 kcal/mol.⁴⁴ As far as we are aware, no experimental values are available for these compounds. By using $\Delta H_f^0(\text{CH}_3\text{OH}) = -45.7$ kcal/mol at 0 K,⁴⁴ the changes in the heat of formation upon CH/CF replacement are -54.1 kcal/mol when going from CH_3OH to CH_2FOH , -59.3 kcal/mol from CH_2FOH to CHF_2OH , and -56.7 kcal/mol from CHF_2OH to CF_3OH . Thus the energy effects of the CH/CF replacement are not quite additive, and the small differences

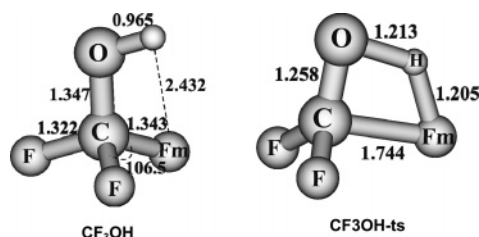


Figure 1. Selected MP2/aVTZ optimized geometry parameters of **CF₃OH** and the transition state structure **CF₃OH-ts** for unimolecular HF-elimination. Bond lengths in Å and bond angles in degrees.

TABLE 4: Calculated Energy Barriers (kcal/mol) for HF-Elimination from Three Fluoromethanols

method ^a	CH ₂ FOH	CHF ₂ OH	CF ₃ OH
MP2/aug-cc-pVDZ ^b	40.3	40.1	41.5
MP2/aug-cc-pVTZ	41.4	41.0	42.3
MP2/aug-cc-pVQZ	41.6	41.2	42.5
MP2/CBS ^c	41.7	41.3	42.6
CCSD(T)/aug-cc-pVDZ	41.2	41.8	43.7
CCSD(T)/aug-cc-pVTZ	42.3	42.7	44.5
CCSD(T)/aug-cc-pVQZ	42.7	42.9	44.8
CCSD(T)/CBS ^d	42.9	43.1	45.0
CCSD(T)/CBS(est eq 3)	42.7	42.9	44.8

^a Based on MP2/aug-cc-pVTZ optimized geometries, unless otherwise noted. Values given including zero-point corrections derived from MP2/aug-cc-pVTZ where O–H stretches were scaled by a factor of 0.9798 and C–H stretches were scaled by a factor of 0.9701. ^b Based on MP2/aug-cc-pVDZ optimized geometries. ^c Based on MP2 energies extrapolated at a complete basis set limit; see text. ^d Based on CCSD(T) energies extrapolated at a complete basis set limit; see text.

are indicative of the additional stabilizing effects induced by *geminal*-F-atoms. The largest increment for forming the difluorinated derivative is due to the H atom being able to form intramolecular bonds with two fluorine ligands instead of only one in CH₂FOH. This effect is manifested also by the emergence of a *gauche* form as the equilibrium structure of CHF₂OH, whereas the FCOH-staggered conformer remains the lowest-lying form in both mono- and trifluorinated methanols. The H...F hydrogen bonds in CHF₂OH and CF₃OH are maximized in a staggered conformation by involvement of two F-atoms. In CH₂FOH, both *cis* and *trans* conformers are characterized by one imaginary frequency, corresponding to the TS's for internal rotation around the C–O bond. The barriers to rotation are 2.5 and 4.0 kcal/mol for the *cis* and *trans* forms, respectively (values at MP2/aVTZ + ZPE). In both CHF₂OH and CF₃OH, the eclipsed *cis*-form is the sole TS for internal rotation, with energy barriers of 2.9 and 0.6 kcal/mol, respectively. The rotation barrier decreases with the increasing the number of F-atoms.

Figure 1 shows the selected MP2/aVTZ optimized parameters of the equilibrium structure of CF₃OH and the corresponding TS for HF-loss, **CF₃OH-ts**. The Cartesian coordinates of the minima and associated TS's of the two product molecules are given in the Supporting Information. In going from CH₂FOH to CF₃OH, the TS geometry is not significantly modified. Each TS exhibits C_s point group symmetry and a four-member ring. The C–F_m distance (m stands for migrating) is substantially stretched from 1.32 Å in the minimum to 1.74 Å in the CF₃OH TS. The O–H bond also lengthens but to a much lesser extent (~0.14 Å). With an H–F distance of 1.205 Å, the departing HF is already partially formed. The C–O distance is shortened by ~0.1 Å to 1.258 Å, close to that in CF₂O, and the CF₂ group approaches planarity.

The energy barriers for HF-elimination in the three F-methanols were calculated at the MP2 and CCSD(T) levels with

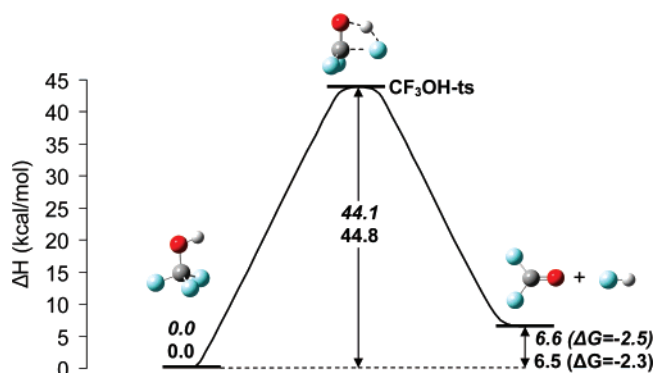


Figure 2. Schematic energy profiles for HF-elimination from the monomer **CF₃OH**. Values in *italic-bold* were obtained from the calculated heats of formation. Relative enthalpies at 0 K were obtained from CCSD(T)/CBS calculations plus corrections (upper values) and the estimated CCSD(T)/CBS (eq 3) + ZPE (lower values). ΔG is free energy of reaction at 298 K. Energies in kcal/mol.

TABLE 5: Activation Enthalpies (kcal/mol), Activation Entropies (cal/(mol K)), and Activation Free Energies (kcal/mol) for HF-Elimination from Three Fluoromethanols

	ΔH [‡] (298 K) ^a	ΔS [‡] ^b	ΔG [‡] (298 K)
CF ₃ OH	44.0	−0.29	44.1
CHF ₂ OH	42.1	0.31	42.0
CH ₂ FOH	43.8	−0.26	43.9

^a Based on the calculated heats of formation at 298 K. ^b From MP2/aVTZ values.

different basis sets (Table 4). Figure 2 illustrates the energy profiles for CF₃OH obtained at the CCSD(T)/CBS level. The barrier for a given path tends to increase on improvement of the correlation treatment or extension of the basis set. Using the CCSD(T)/CBS values, the barrier height increases slightly but regularly within the F-methanol series from the mono- (42.9 kcal/mol) to the di- (43.1 kcal/mol) to the trifluoro derivative (45.0 kcal/mol). For CF₃OH, our barrier of 45.0 kcal/mol is the same as the value at the G3//B3LYP level,⁸¹ very close to the value of 45.1 ± 2 kcal/mol obtained at the QCISD(T)/6-311G(2df,2p) + ZPE level,¹¹ and is at the upper limit of 42 ± 3 kcal/mol predicted from MP4/TZ2P + ZPE calculations.¹² The MP4 result is closer to our MP2 values of 42.2–42.5 kcal/mol (Table 4). We can also use the results for the monomeric transition states to see how well our approximation, given in eq 3 to estimate the barriers for the dimers, will work. Use of the MP2 method, as shown in eq 3, for estimating the energy differences needed for the extrapolation of the CCSD(T)/aVTZ values to the CBS limit, shows that this will introduce errors on the order of 0.2 kcal/mol.

The calculated entropies and Gibbs free energies at 298 K are given in Table 5. The activation entropy is small and negative, ΔS[‡] = −0.26 and −0.29 cal/(mol K), in CH₂FOH and CF₃OH, respectively, and small but positive ΔS[‡] = 0.31 cal/(mol K) in CHF₂OH. These small values are consistent with a transition state that has approximately the same size of the degrees of freedom as the reactants.

Bimolecular HF-Elimination from Trifluoromethanol.

Although a variety of H-bonded dimers could be expected from interactions between the OH and CF groups of two monomers, only cyclic dimers are relevant as pre-association complexes leading to loss of HF. We were able to locate two distinct types of cyclic dimers, **dim-6** and **dim-8**, whose selected MP2/aVTZ optimized geometries are displayed in Figure 3. The full Cartesian coordinates are listed in the Supporting Information.

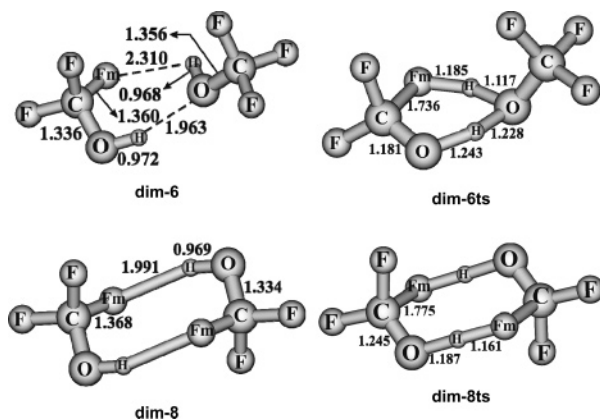


Figure 3. Selected MP2/aVTZ geometry parameters of two dimers **dim-6** and **dim-8** of CF₃OH, and the TS's for HF-elimination **dim-6ts** and **dim-8ts**. Bond lengths in Å and bond angles in degrees.

dim-6 corresponds to a six-membered cyclic complex involving a *cis*-FCOH framework of one monomer with the O—H bond of another monomer. This dimer was previously studied by Doering et al. at the HF, MP2, and B3LYP levels with basis sets ranging from 6-311++G(d,p) to 6-311++G(2d,2p).¹⁷ Within the nearly planar six-member ring, two different hydrogen bonds due to O—H...O and C—F_m...H interactions are found. The intermolecular O...H distance of 1.963 Å is longer than that of ~1.90 Å for the O—H...O bond in the open-chain dimer of methanol.¹⁷ The F_m...H distance of 2.310 Å is substantially longer than the O—H...O distance. The C—O distance involved in the interacting *cis*-F_mCOH framework decreases by 0.01 Å (1.336 Å), whereas the other C—O bond in the dimer increases by a similar amount (1.356 Å), with respect to that in the monomer (1.347 Å, Figure 1). This suggests substantial charge reorganization in both monomers.

We investigated a planar structure in which each proton is H-bonded to two F atoms with *C*_{2h} symmetry. The MP2/aVDZ electronic energy of this structure is 1.0 kcal/mol higher with respect to the lowest energy dimer, **dim-8**, and 0.6 kcal/mol higher if the scaled ZPEs are included. However, it has two imaginary frequencies, 82.8i and 37.2i, both of them showing distortions from *C*_{2h} to *C*_i symmetry (as that of **dim-8**).

We have also located for the first time a second dimer, **dim-8**, which is a nearly planar eight-member ring formed by two F_mCOH frameworks having *C*_i point group symmetry. The intermolecular F_m...H distance of 1.991 Å is substantially shorter than that in **dim-6**, and the C—F_m, C—O, and O—H bond distances remain almost unchanged (changes <0.01 Å) with respect to the F_mCOH framework in **dim-6**. Both dimers, **dim-6** and **dim-8**, are calculated to have comparable complexation energies, with the former more stable by less than 0.3 kcal/mol at the estimated CCSD(T)/CBS limit. At the CCSD(T)/aug-cc-pVTZ level, **dim-8** is slightly more stable than **dim-6**.

Figure 4 shows the schematic energy profiles for loss of HF or two HF from the dimers **dim-6** (Figure 4a) and **dim-8** (Figure 4b). **dim-6** is the pre-association starting point for generating one HF molecule, and rearrangement of **dim-8** gives rise to two HF molecules. In a way similar to that described above for decomposition of the monomer, we can evaluate the thermodynamics for the HF elimination from the dimers (in kcal/mol) using the estimated CCSD(T)/CBS energies and MP2/aVTZ entropies and thermal corrections (MP2/aVDZ for the dimers):

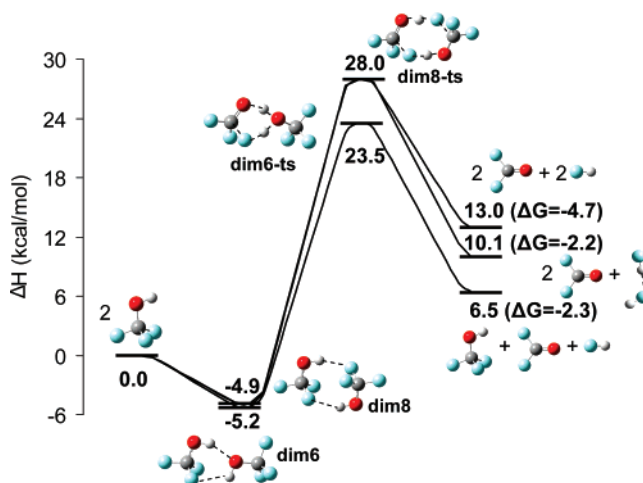
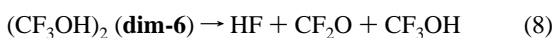


Figure 4. Schematic energy profiles showing the HF-elimination pathways from dimers **dim-6** and **dim-8**. Relative enthalpies at 0 K were obtained from estimated CCSD(T)/CBS (eq 3) + ZPE calculations. ΔG is free energy of reaction at 298 K. Energies in kcal/mol.

At 298 K, ΔH(R8) = 12.5 kcal/mol, ΔG(R8) = -5.9 kcal/mol, ΔH(R9) = 20.2 kcal/mol, and ΔG(R9) = -9.5 kcal/mol. Again the reactions have positive enthalpies and negative free energies. The corresponding TS's, **dim-6ts** and **dim-8ts**, for these eliminative processes are also shown in Figure 3. TS **dim-6ts** is compact with a quasi planar six-ring, in which all of the bonds are either stretched or compressed. The most important change is the C—F_m bond distance. The distance of 1.185 Å in the departing H—F_m is quite short, and the H remains strongly bonded to its O. The transferred H-atom between the two oxygen centers is marginally closer to the accepting atom. The C—O bond within the six-ring is shortened with substantial double bond character. **dim-6ts** is 23.5 kcal/mol above the separated monomers (CF₃OH)₂ and 28.7 kcal/mol above **dim-6** (Figure 4a). The barrier height for HF-elimination from the dimer **dim-6** is 16.3 kcal/mol below that for the unimolecular decomposition of CF₃OH (45.0 kcal/mol).

dim-6ts is similar to the TS involved in CF₃OH decomposition assisted by a water molecule. For the H₂O assisted process, Schneider et al.,¹² using MP4/TZ2P calculations, reported an energy barrier of ~17 kcal/mol with respect to the separated CF₃OH + H₂O reactants. No pre-association complex was located by these authors. The reported MP4 value could be underestimating the true barrier height by a few kcal/mol, because incorporation of a larger amount of electron correlation in the wavefunctions tends to increase the barrier height (cf. Table 6).

dim-8 undergoes decomposition through **dim-8ts** yielding simultaneously two HF molecules. This TS (Figure 3) maintains *C*_i symmetry with a nearly planar ring and has a shorter HF_m distance but a longer CF_m bond. The C—O distance of 1.245 Å is longer than that in **dim-6ts**. **dim-8ts** is calculated to be 28.0 kcal/mol above the monomers, giving an energy barrier of 32.9 kcal/mol for the decomposition **dim-8** → **dim-8ts** (Figure 4b). Both bimolecular processes are energetically favorable as compared to the unimolecular process. **dim-8ts** is 4.5 kcal/mol higher in energy than **dim-6ts**, suggesting a preference for the loss of one-HF from dimeric trifluoromethanol.

HF-Elimination from Trifluoromethanol Catalyzed by Hydrogen Fluoride. We now consider the catalytic effect of at least one HF molecule on the HF elimination paths. Table 7 lists the relative energies of the complexes and transition states obtained at both MP2 and CCSD(T) levels using the aVTZ basis

TABLE 6: Energies Related to the HF-Elimination from the Trifluoromethanol Dimers Calculated at Different Levels of MO Theory^a

method	2(CF ₃ OH)	dim-6 ^b	dim-6ts ^b	dim-8 ^b	dim-8ts ^{b,c}
MP2/aVDZ ^c	0.00	-7.0	17.4	-7.5	19.5
MP2/aVTZ	0.00	-5.6	19.3	-5.6	22.9
MP2/aVQZ	0.00	-5.2	20.3	-5.1	24.0
MP2/CBS	0.00	-5.0	20.9	-4.9	24.7
CCSD(T)/aVDZ	0.00	-6.2	20.8	-6.8	23.7
CCSD(T)/aVTZ	0.00	-5.7	21.8	-5.9	26.2
CCSD(T)/CBS(eq 3) ^d	0.00	-5.2	23.5	-4.9	28.0

^a Based on MP2/aVTZ optimized geometries, unless otherwise noted.

^b Relative energies with respect to the two separated monomers, including zero-point corrections. ZPE's were obtained from MP2/aVDZ harmonic vibrational frequencies and those corresponding to a O-H stretching were scaled by a factor of 0.9798. ^c Based on MP2/aVDZ optimized geometries. ^d Estimated by using eq 3.

sets. These components were used to evaluate the final CCSD(T)/CBS energies based on eq 3.

Figure 5 displays a selection of MP2/aVTZ optimized geometrical parameters of the corresponding initial complexes **CF₃OH-HF** and **CF₃OH-2HF**, and TS's **CF₃OH-HFts** and **CF₃OH-2HFts**, that include one CF₃OH monomer plus one and two HF molecules, respectively. The Cartesian coordinates are given in the Supporting Information. To facilitate the comparison, Figure 6 shows the schematic potential energy profiles for both reaction paths obtained at the approximate CCSD(T)/CBS level.

We consider only the closed complex **CF₃OH-HF**, which is a six-member cycle containing two hydrogen bonds, OH-F and F_m-HF. Though the OH-FH-F_m framework is nearly planar ($\angle\text{HFHF}_m$ dihedral angle of 5.7°), the CF₂ group is strongly puckered ($\angle\text{F}_m\text{COH}$ dihedral angle of 54.0°) in such a way that the alcohol molecule avoids the energetically less favorable eclipsed conformation. The intermolecular H-F distance of 1.941 Å is shorter than the H-F_m distance of 2.229 Å, likely due to the stronger inductive effect of the oxygen atom (Figure 5). **CF₃OH-HF** is more stable than the separated reactants by 4.2 kcal/mol, slightly larger than the binding energy of 2.9 kcal/mol for the dimer (HF)₂ at the same level.

The geometry of **CF₃OH-HFts** tends to be more compact and closer to planarity, with dihedral angles of only ~5–8°. Except for the C-F_m distance of 1.750 Å, the remaining bonds are in the range of 1.14–1.24 Å. The three different H-F bond distances for **CF₃OH-HFts** are 1.165, 1.149, and 1.142 Å, which are similar to those of 1.136 Å predicted¹⁵ in the TS for the HF trimer (*D*_{3h} symmetry) at the HF/TZVP level. Each of the two transferring H-atoms is situated approximately in the middle of the O...F or F...F nonbonded interactions. In many aspects, the shape of this TS is similar to that of **dim-6ts** discussed above, in which the OCF₃ group is now replaced by an F atom. It can also be compared to the TS related to the (HF)₃ trimer.¹⁵

The two HF-molecules that are formed as products from the **CF₃OH-HFts** could be either fully separated from each other or form an (HF)₂ dimer (Figure 6a). Relative to the initial complex, the energy barrier for the path **CF₃OH-HF** → **CF₃OH-HFts** is calculated to be 26.1 kcal/mol (Table 7, Figure 6a). This is a reduction of 2.6 kcal/mol for the barrier height with respect to that of 28.7 kcal/mol calculated for the bimolecular pathway **dim-6** → **dim-6ts** (cf. Figure 4). Again, the free energy of reaction (ΔG_r) becomes negative (Figure 6a).

We now consider the elimination process involving the participation of two HF-molecules in the supermolecule. This path is initiated by the pre-association complex **CF₃OH-2HF**

and proceeds through the TS **CF₃OH-2HFts** (Figure 5). In the eight-member cyclic complex **CF₃OH-2HF**, the four heavy atoms O-F-F-F_m basically form a plane. The three migrating H atoms are situated almost in the plane (out-of-plane distortion of ~2°), the C(F₂) group is again puckered, but to a lesser extent than in the previous case with the $\angle\text{F}_m\text{COH}$ dihedral angle being ~38°. This complex contains one O-H-F and two F-H-F hydrogen bonds and is characterized by much shorter intermolecular H-F distances (~1.68–1.80 Å) as compared to those in **CF₃OH-HF**.

The geometric features of **CF₃OH-2HF** are consistent with a large complexation energy of 11.6 kcal/mol, relative to the separated monomers (Figure 6b). Compared with complexation energies of 2.9 kcal/mol for the dimer (HF)₂ and 4.2 kcal/mol for **CF₃OH-HF** (Figure 6a), the value of 11.6 kcal/mol is more than the sum of the two values that correspond to the same number of H-bonds (three). The (HF)₃ trimer has a complexation energy of 10.5 kcal/mol comparable to that of **CF₃OH-2HF**.

In the TS **CF₃OH-2HFts**, the atoms F-H-F-H-F_m form a planar framework, from which the other moiety, including the C atom, is only marginally out-of-plane. Similar to **CF₃OH-HFts**, only the leaving C-F_m distance is relatively long (1.769 Å), whereas the remaining distances are again in the range 1.13–1.24 Å. Each H-atom is located nearly at the midpoint between the two connected heavy atoms, and the O-H-F and F-H-F groups are close to linear. These geometry changes suggest a relatively low-energy H-transfer leading to HF elimination. **CF₃OH-2HFts** is calculated to be 8.7 kcal/mol higher in energy than the separated fragments and 20.3 kcal/mol higher in energy than the complex **CF₃OH-2HF**. The calculated free energy of HF elimination depends on the number of products that are formed. When the (HF)₃ trimer is formed, the free energy ΔG_r is no longer negative, but the reaction enthalpy ΔH_r is negative, relative to the reactant fragments. The results show that the active participation of HF in the reaction pathway results in a substantial reduction of the energy barrier for HF-elimination from CF₃OH with respect to that of the monomer. The (HF)₂ dimer is a better catalyst than the HF monomer.

HF-Elimination from Trifluoromethanol Dimer Catalyzed by Hydrogen Fluoride. The energy barrier for HF elimination is reduced in the (CF₃OH)₂ dimer or by additional catalytic HF. We thus examined if the combination of both effects, processes involving two CF₃OH plus one and two HF molecules, would lead to further reductions in the barrier. Figure 7 displays MP2/aVTZ optimized geometrical parameters of the relevant structures, and Figure 8 gives the potential energy profiles illustrating the reaction pathways.

dim-HF is found to be the energetically lowest-lying cyclic complex formed from interaction of two CF₃OH molecules and one HF molecule. This structure is derived from **dim-6**, the most stable CF₃OH dimer with HF inserted into the F_m-H bond. The resulting trimer retains the existing strong OH-O hydrogen bond and adds a strong H-FH hydrogen bond. As in the other complexes, the four O-O-F-F atoms within the eight-member ring form a plane, from which the H-atoms are marginally distorted. The C(F₂) is substantially out of the plane, characterized by a dihedral $\angle\text{FCOH}$ angle of ~68°. The intermolecular distances of 1.77–1.82 Å in **dim-HF** are comparable to those in **CF₃OH-2HF**. The similarity between both trimers is also found for the complexation energy, which is 11.8 kcal/mol for **dim-HF** relative to three separated monomers.

Starting from **dim-HF**, the HF elimination channel passes through the TS **dim-HFts**, whose geometric features are similar to those of **CF₃OH-2HFts**. The TS **dim-HFts** contains a nearly

TABLE 7: Relative Energies Related to HF-Eliminations from Trifluoromethanol Monomer and Dimers with HF^a

separated system ^b	structure ^c	MP2/ aVDZ ^d	MP2/ aVTZ	MP2/ aVQZ	MP2/ CBS	CCSD(T)/ aVDZ	CCSD(T)/ aVTZ	CCSD(T)/ CBS ^e
CF ₃ OH + HF	CF ₃ OH–HF (complex) ^f	−5.1	−4.3	−4.1	−3.9	−4.8	−4.5	−4.2
	CF ₃ OH–HFts (TS) ^f	17.9	18.6	19.3	19.7	20.7	20.7	21.9
CF ₃ OH + 2HF	CF ₃ OH–2HF (complex)	−12.9	−12.0	−11.6	−11.3	−12.8	−12.3	−11.6
	CF ₃ OH–2HFts (TS)	4.2	4.2	5.5	6.4	7.2	6.5	8.7
2CF ₃ OH + HF	dim-HF (complex)	−14.6	−12.6	−11.9	−11.6	−13.4	−12.8	−11.8
	dim-HFts (TS)	4.2	5.7	7.3	8.3	7.9	8.4	11.0
2CF ₃ OH + 2HF	dim-2HF (complex)	−19.7	−17.3	−16.4	−15.9	−19.3	−17.8	−16.4
	dim-2HFts (TS)	7.0	9.1	11.1	12.4	11.8	12.8	16.1

^a Based on MP2/aVTZ optimized geometries. ZPE's were obtained from MP2/aVDZ harmonic vibrational frequencies and those corresponding to an O–H stretch were scaled by a factor of 0.9823, unless otherwise noted. ^b Relative energies are given with respect to the corresponding separated system, including zero-point corrections. ^c Labeling of structures given in Figures 5 and 7. ^d Based on MP2/aVDZ optimized geometries. ^e Estimated by using eq 3. ^f ZPE's were obtained from MP2/aVTZ harmonic vibrational frequencies and those corresponding to an O–H stretch were scaled by a factor of 0.9798.

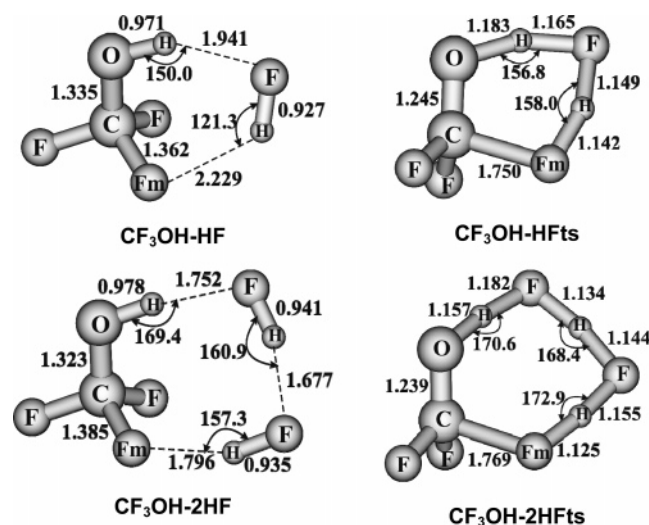


Figure 5. Selected MP2/aVTZ geometry parameters of the complexes **CF₃OH–HF** and **CF₃OH–2HF** and the corresponding TS's for HF-elimination **CF₃OH–HFts** and **CF₃OH–2HFts**. Bond lengths in Å and bond angles in degrees.

planar OOFF ring in which the H atom transfer occurs almost collinear between the lone pairs of the two connected heavy atoms. Two HF molecules and one CF₃OH molecule are formed as products. **dim-HFts** is 22.8 kcal/mol higher in energy than the trimer, but only 11.0 kcal/mol higher in energy than the reactant fragments (Figure 8). The energy barrier for HF-elimination from **dim-HF** is ~2.5 kcal/mol larger than the barrier starting from **CF₃OH–2HF**. Liedl et al.⁸² found that the energy barriers for proton transfer in (HF)_x, with *x* = 3, 4, or 5, are lower than those for (H₂O)_x. CF₃OH should be similar to H₂O, so this result is consistent with the fact that HF is a better catalyst.

Addition of a second HF molecule to **dim-HF** could give rise to a number of open and cyclic tetrameric complexes. We selected the **dim-2HF** structure shown in Figure 7 as a representative tetramer, which serves as a pre-association point for HF-elimination. A particular feature of **dim-2HF** is the alternating position between CF₃OH and HF entities in which all the heavy atoms take part in the complex. This structure can be regarded as a dimer of the (CF₃OH–HF) dimer. Another possible tetramer combines the two dimers (CF₃OH)₂ and (HF)₂, which leads to a CF₃ group outside the cyclic framework as in **dim-HF**. The twelve-member cycle **dim-2HF** has *C_i* point group symmetry with relatively short intermolecular F–H distances of ~1.74 Å. Due to the molecular symmetry, the O–F(HF)–

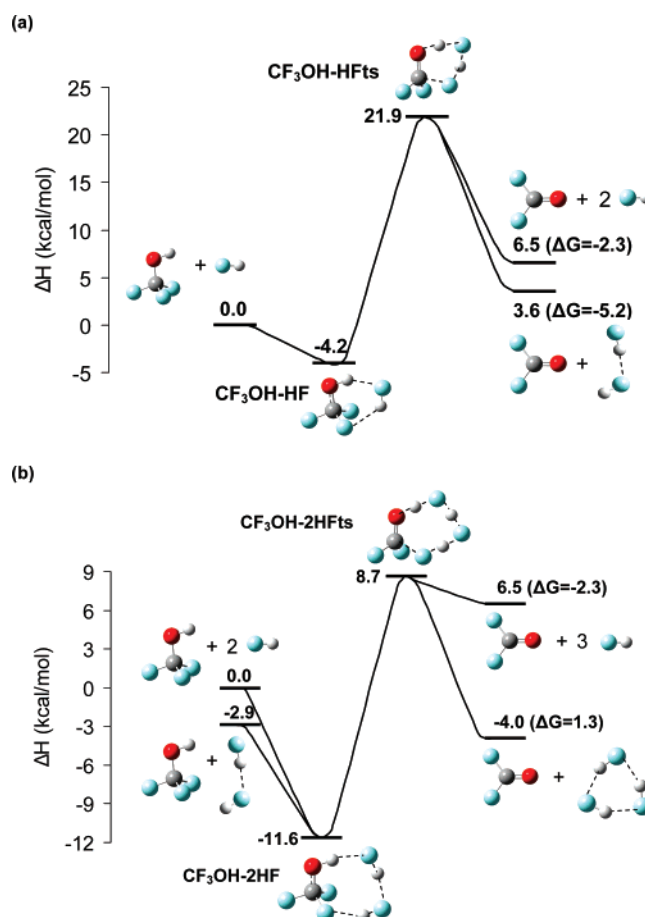


Figure 6. Schematic energy profiles for HF elimination from CF₃OH with (a) one HF and (b) two HF molecules. Relative enthalpies at 0 K were obtained from estimated CCSD(T)/CBS (eq 3) + ZPE calculations. ΔG is free energy of reaction at 298 K. Energies in kcal/mol.

O–F(HF) framework is strictly planar. The tetramer has a complexation energy of 16.4 kcal/mol relative to the separated monomers.

dim-2HFts maintains the *C_i* symmetry with approximately linear O–H–F and F–H–F moieties. Similar to **dim-8ts**, **dim-2HFts** leads to the formation of 2HF from 2CF₃OH. **dim-2HFts** is calculated to be 16.1 and 32.5 kcal/mol higher in energy than the separated monomers and **dim-2HF**, respectively (Figure 8). This barrier height makes this tetramer route less competitive as compared to the various dimer and trimer channels discussed above.

Kinetics of the Decomposition Mechanism. Table 8 lists the rate constants calculated using TST and RRKM theory; 3-D

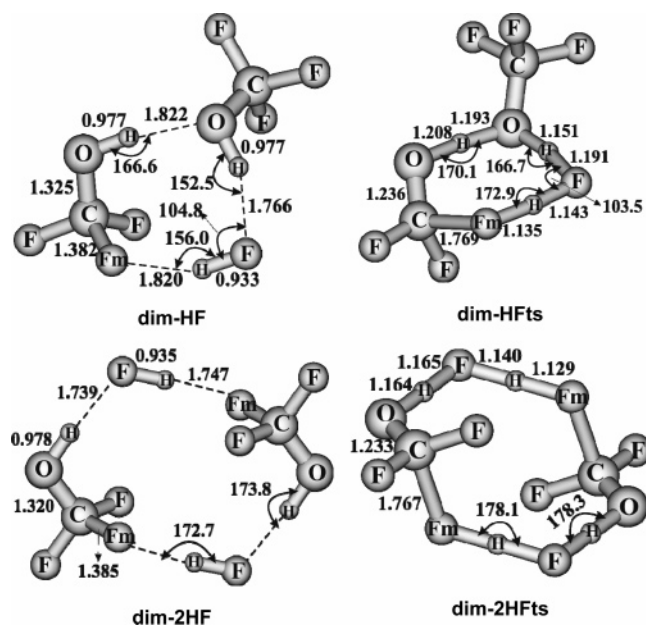


Figure 7. Selected MP2/aVTZ geometry parameters of the complexes involving two CF_3OH molecules with HF, **dim-HF** and **dim-2HF**, and the TS's for HF-elimination, **dim-HFts** and **dim-2HFts**. Bond lengths in Å and bond angles in degrees.

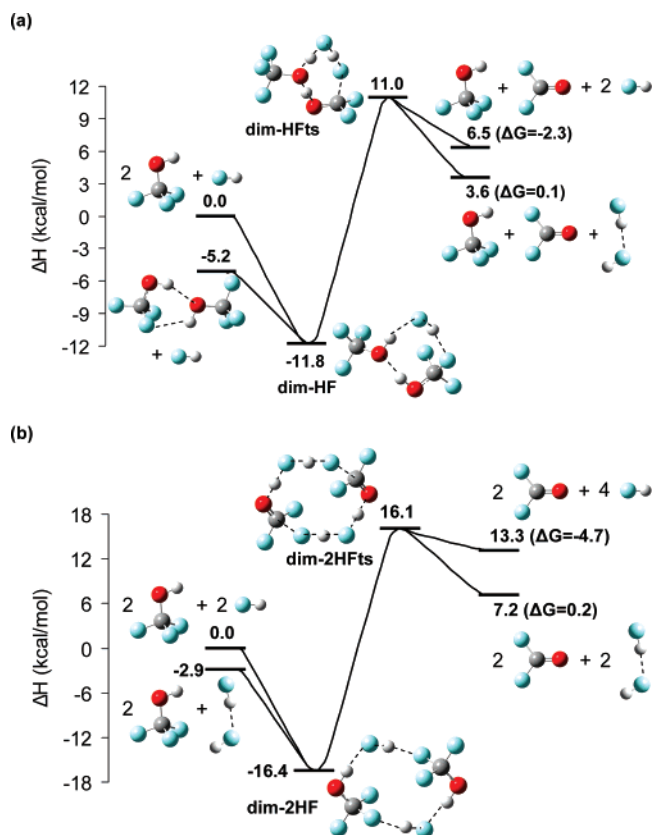
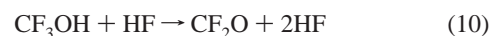


Figure 8. Schematic energy profiles for HF elimination from two CF_3OH molecules with (a) one HF and (b) two HF molecules. Relative enthalpies at 0 K were obtained from estimated CCSD(T)/CBS (eq 3) + ZPE calculations. ΔG is free energy of reaction at 298 K. Energies in kcal/mol.

plots of the rate coefficients are given in Figure 9. HF-loss in an isolated CF_3OH monomer is predicted to be extremely slow at room temperature, but becomes substantial at 500 K. For the decomposition of this monomer (eq 7), we obtain corrected rate constants of $k_\infty(298 \text{ K}) = 2.20 \times 10^{-13} \text{ s}^{-1}$ and $k_\infty(500 \text{ K}) =$

$8.57 \times 10^{-7} \text{ s}^{-1}$, showing that this reaction is very slow. For the mono-HF elimination from a dimer (**dim-6**, eq 8), TST predicts $k_\infty(298 \text{ K}) = 9.10 \times 10^{-9} \text{ s}^{-1}$ and $k_\infty(500 \text{ K}) = 5.52 \times 10^{-2} \text{ s}^{-1}$, including tunneling corrections. Treating this reaction as a bimolecular process with two CF_3OH reactant molecules, we obtain a TST rate constant of $k_\infty(298 \text{ K}) = 1.29 \times 10^1 \text{ cm}^3/(\text{mol s})$ and $k_\infty(500 \text{ K}) = 6.67 \times 10^3 \text{ cm}^3/(\text{mol s})$. Thus, this reaction will be much faster than reaction 7. In the case of the di-HF elimination from **dim-8** (eq 9), the TST rate constant expression is $k_\infty(298 \text{ K}) = 7.22 \times 10^{-13} \text{ s}^{-1}$ including tunneling corrections, which is very slow.

We calculated the rate constants for reactions where HF is used as autocatalyst:



For reaction 10 we obtained from bimolecular TST $k_\infty(298 \text{ K}) = 1.20 \times 10^1 \text{ cm}^3/(\text{mol s})$, including tunneling ($Q_{\text{ST}} = 1.10 \times 10^2$). If the tunneling is calculated for the $\text{CF}_2\text{O} + (\text{HF})_2$ products we obtained a slightly larger value for $Q_{\text{ST}} = 1.80 \times 10^2$, and a larger rate constant of $k_\infty(298 \text{ K}) = 1.96 \times 10^1 \text{ cm}^3/(\text{mol s})$. If we take the complex **CF₃OH–HF** as the reactant for reaction 10, we obtain the unimolecular TST rate constant expression including tunneling of $k_\infty(298 \text{ K}) = 7.57 \times 10^{-6} \text{ s}^{-1}$ for the separated products and $k_\infty(298 \text{ K}) = 1.22 \times 10^{-5} \text{ s}^{-1}$ with HF dimer as a product (see Table 8). Thus the reaction starting from separated reactants would be expected to be quite fast but if the complex is formed, it is much slower. Reaction 11 as a bimolecular reaction has a TST rate constant of $k_\infty(298 \text{ K}) = 1.79 \times 10^6 \text{ cm}^3/(\text{mol s})$, including a tunneling correction of $Q_{\text{ST}} = 8.54$. In the case of the complex, **CF₃OH–2HF**, the TST rate constant is $k_\infty(298 \text{ K}) = 1.56 \times 10^{-2} \text{ s}^{-1}$ including tunneling. Thus, even if the complex is formed, the reaction will still be quite fast. For reaction 12, the bimolecular reaction $(\text{CF}_3\text{OH})_2$ as a reactant (**dim-6**), we obtain the TST rate constant of $k_\infty(298 \text{ K}) = 1.54 \times 10^{-1} \text{ cm}^3/(\text{mol s})$ with tunneling and separated reactants and with the HF dimer as a product, $k_\infty(298 \text{ K}) = 2.70 \times 10^{-1} \text{ cm}^3/(\text{mol s})$. For reaction 12 starting from the **dim-HF** complex, we calculate the unimolecular TST rate constant of $k_\infty(298 \text{ K}) = 1.69 \times 10^{-4} \text{ s}^{-1}$ if separated products are considered for the tunneling calculation, and $k_\infty(298 \text{ K}) = 2.13 \times 10^{-4} \text{ s}^{-1}$ if the HF dimer is considered for the tunneling (see Table 8). In all of these processes (eqs 7–12), the values found by RRKM for the rate constants at 298 K are the same at 1 and 11 atm; therefore, the limit of high pressure is already reached at 1 atm. The rate constants show that reactions 8 and 10–12 are all potential paths for CF_3OH decomposition with reaction 11 being the most likely. If we use the RRKM rate constant at 298 K, $k(298 \text{ K}) = 1.76 \times 10^{-2} \text{ s}^{-1}$ for reaction 11, we calculate the half-life for CF_3OH in the gas phase as less than 1 min (39 s) when CF_3OH or HF are present at reasonable pressures.

Electronic Mechanism of the Decomposition. Each of the TS's **dim-6ts**, **CF₃OH–HFts**, **CF₃OH–2HFts**, **dim-HFts**, and **dim-2HFts**, has the character of a catalytic process. By donating an H-atom to form HF and receiving another H-atom back, the second CF_3OH monomer and/or HF-molecules remain intact (with different H atoms) and act as a bifunctional acid–base catalyst facilitating H-transfer. **dim-8ts** is a concerted elimination in which HF formation is accelerated by passing through a cyclic TS. The F atom of one monomer receives the H atom of the

TABLE 8: Rate Constants $k(T)$ Obtained by TST and RRKM Theory at Different Temperatures (in Kelvin) Including Tunneling Corrections (Q_{ST})^a

reaction	T	$Q_{ST}(T)$	TST	RRKM
$\text{CF}_3\text{OH} \rightarrow \text{CF}_3\text{OH-ts} \rightarrow \text{CF}_2\text{O} + \text{HF}$	298.15	3.46×10^7	$k_\infty(T) = 7.94 \times 10^{11} T^{0.45} \exp(-45.2/RT) \text{ s}^{-1}$	$k(T,p) = 2.00 \times 10^{11} p^{0.42} \exp(-44.8/RT) \text{ s}^{-1}$
	500	4.22	2.20×10^{-13} 8.57×10^{-7}	2.06×10^{-13} 7.93×10^{-7}
$2\text{CF}_3\text{OH} \rightarrow \text{dim-6ts} \rightarrow \text{CF}_3\text{OH} + \text{CF}_2\text{O} + \text{HF}$	298.15	1.10×10^2	$k(T) = 2.25 T^{3.17} \exp(-12.5/RT) \text{ cm}^3/(\text{mol s})$	
	500	2.28	1.29×10^1 6.67×10^3	
$\text{dim-6} \rightarrow \text{dim-6ts} \rightarrow \text{CF}_3\text{OH} + \text{CF}_2\text{O} + \text{HF}$	298.15	1.10×10^2	$k_\infty(T) = 1.58 \times 10^{10} T^{0.18} \exp(-28.2/RT) \text{ s}^{-1}$	$k(T,p) = 8.71 \times 10^9 p^{0.21} \exp(-28.0/RT) \text{ s}^{-1}$
	500	2.28	1.06×10^{-8} 5.52×10^{-2}	1.29×10^{-8} 6.36×10^{-2}
$\text{dim-8} \rightarrow \text{dim-8ts} \rightarrow 2 \text{ CF}_2\text{O} + 2\text{HF}$	298.15	5.15	$k_\infty(T) = 2.51 \times 10^{10} T^{0.37} \exp(-32.9/RT) \text{ s}^{-1}$	$k(T,p) = 5.01 \times 10^{10} p^{0.19} \exp(-33.0/RT) \text{ s}^{-1}$
	500	1.56	7.26×10^{-13} 1.51×10^{-3}	7.20×10^{-13} 1.49×10^{-3}
$\text{CF}_3\text{OH} + \text{HF} \rightarrow \text{CF}_3\text{OH-HFts} \rightarrow \text{CF}_2\text{O} + 2\text{HF}$	298.15	1.10×10^2	$k(T) = 2.14 \times 10^4 T^{2.04} \exp(-14.2/RT) \text{ cm}^3/(\text{mol s})$	
	500	2.35	1.20×10^1 1.11×10^4	
$\text{CF}_3\text{OH-HF} \rightarrow \text{CF}_3\text{OH-HFts} \rightarrow \text{CF}_2\text{O} + 2\text{HF}$	298.15	2.19×10^2	$k_\infty(T) = 5.01 \times 10^{11} T^{-0.21} \exp(-25.5/RT) \text{ s}^{-1}$	$k(T,p) = 5.88 \times 10^9 p^{0.32} \exp(-24.9/RT) \text{ s}^{-1}$
	500	2.35	7.57×10^{-6} 2.56	8.73×10^{-6} 2.85
$\text{CF}_3\text{OH} + (\text{HF})_2 \rightarrow \text{CF}_3\text{OH-2HFts} \rightarrow \text{CF}_2\text{O} + 3\text{HF}$	298.15	8.54	$k(T) = 5.49 \times 10^8 T^{2.15} \exp(-2.41/RT) \text{ cm}^3/(\text{mol s})$	
	500	1.91	1.79×10^6 5.74×10^6	
$\text{CF}_3\text{OH-2HF} \rightarrow \text{CF}_3\text{OH-2HFts} \rightarrow \text{CF}_2\text{O} + 3\text{HF}$	298.15	2.28×10^1	$k_\infty(T) = 1.26 \times 10^{12} T^{-0.32} \exp(-19.8/RT) \text{ s}^{-1}$	$k(T,p) = 3.47 \times 10^9 p^{0.37} \exp(-19.0/RT) \text{ s}^{-1}$
	500	1.96	1.56×10^{-2} 8.30×10^2	1.76×10^{-2} 9.16×10^2
$\text{dim-6} + \text{HF} \rightarrow \text{dim-HFts} \rightarrow \text{CF}_3\text{OH} + \text{CF}_2\text{O} + 2\text{HF}$	298.15	8.37	$k(T) = 7.08 \times 10^2 T^{2.01} \exp(-13.1/RT) \text{ cm}^3/(\text{mol s})$	
	500	1.96	1.54×10^{-1} 7.24×10^2	
$\text{dim-HF} \rightarrow \text{dim-HFts} \rightarrow \text{CF}_3\text{OH} + \text{CF}_2\text{O} + 2\text{HF}$	298.15	3.98×10^1	$k_\infty(T) = 6.31 \times 10^{10} T^{0.019} \exp(-22.2/RT) \text{ s}^{-1}$	$k(T,p) = 5.37 \times 10^9 p^{0.26} \exp(-21.7/RT) \text{ s}^{-1}$
	500	2.05	1.69×10^{-4} 3.28×10^1	1.94×10^{-4} 3.66×10^1

^a RRKM results are at 1 atm of p . The rate constants at 298.15 and 500 K include the tunneling correction.

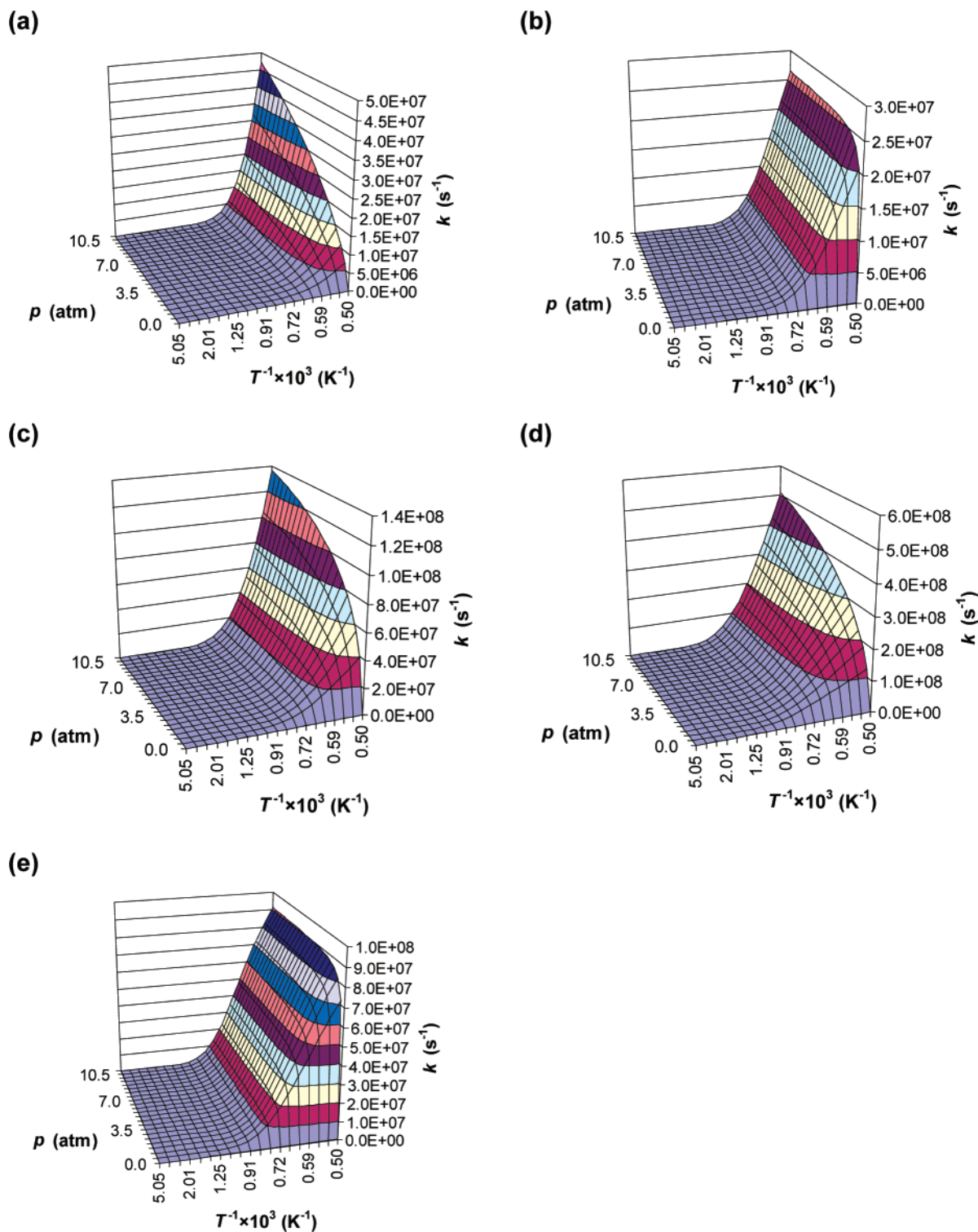


Figure 9. 3-D plots of the rate coefficients k using the RRKM method with N_2 as the bath gas in the temperature range (T) from 200 to 2000 K and pressure range (p) from 0.1 to 8360 Torr. Tunneling corrections are not included. (a) HF elimination from CF_3OH . (b) HF elimination from **dim-6**. (c) 2 HF elimination from CF_3OH with HF as autocatalyst. (d) 3 HF elimination from CF_3OH with HF as autocatalyst. (e) 2 HF Elimination from CF_3OH dimer with HF as autocatalyst.

other monomer. Because both CF_3OH molecules eliminate HF, the process via **dim-8ts** does not have formal catalytic character just as found for $(HF)_3$.¹⁵

To gain additional insight into the electronic reorganization accompanying loss of HF, we analyzed the topology of the electronic densities of the TS's using the atoms-in-molecules (AIM)⁸³ and the electron localization function (ELF)⁸⁴ approaches.⁸⁵ According to the AIM analysis, a bond critical point

(BCP) is characterized by having a minimum value in the electron density along the maximum electron density path connecting two nuclei and is a maximum in all other directions. The appearance of a BCP usually indicates the existence of a chemical bond. The ELF analysis is widely used as a graphical description of the molecular electronic space, which is partitioned into volumes called basins. The ELF value of a basin is always in the range of [0:1], and the higher the ELF value, the

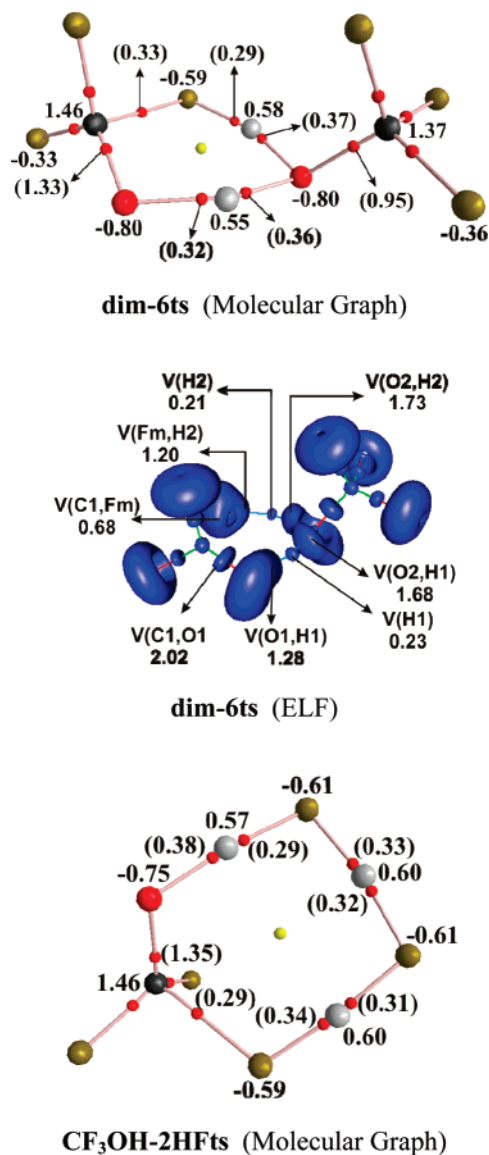


Figure 10. Molecular graphs of **dim-6ts** and **CF₃OH-2HFts**, and the ELF isosurface (ELF = 0.82 au) of **dim-6ts** were constructed from HF/aug-cc-pVTZ wave functions. Black sphere represents C atom, red sphere O, yellow sphere F, gray sphere H, red point bond critical point, and yellow point ring critical point. NBO charges and Wiberg bond indices (given in parentheses) were obtained at the same level.

more localized the density. In the present work, both AIM and ELF calculations were performed using HF/aug-cc-pVTZ wave functions to generate the electron densities; NBO atomic charges were also calculated at the same level.

The graphical representation of ELF provides a qualitative picture of the type of bonds in a molecule and the regions of space where electron pairs are predicted to be. Moreover, the integrated electron density, the average electron population of basin, provides more quantitative information about chemical bonds. The results show that all the of TS's exhibit similar electronic distribution. Figure 10 displays the molecular graphs, atomic charges and bond indices, and the isosurface of ELF = 0.81 (high localization) of the bimolecular TS **dim-6ts** and trimolecular TS **CF₃OH-2HFts** as examples. The electron population of each basin (the integrated electron density over the basin) is also included in the images. In the ELF isosurfaces, we labeled only basins related to the character of the corresponding TS. For **dim-6ts**, the network of BCP's and associated bond orders shown in Figure 10 suggests that within the six-

ring, all bonds are partially broken or partially formed. The departing HF_m group is defined by a BCP, and a bond order of 0.29. The C and H-atoms are positively charged whereas the F_m and O atoms are negatively charged. Each H atom connects two highly electronegative atoms and induces strongly polarized bonds toward opposite directions. The transferred H-atoms can be regarded as protons between O and F_m and between O centers that behave as protonation sites. Thus, the cyclic motion within the six-member ring involves two protonations leading to the formation of two new chemical bonds.

The ELF populations displayed in Figure 10 indicate the existence of 10 core basins [V(C₁), V(C₂), V(O₁), V(O₂), and 6 V(F)] with slightly more than 2 electrons per basin. Each F-atom (except for F_m) has ~6.5 electrons, corresponding to 3 electron pairs coming from three large-volume monosynaptic basins. The O₁ atom possesses two large monosynaptic basins with ~4.5 electron and two valence basins V(C₁,O₁), (O₁,H₁) with average populations of 2.02 and 1.28 electron, respectively. The electron population of 1.28 in the O₁-H₁ basin suggests that the O₁-H₁ bond is nearly half broken. O₂ possesses only one monosynaptic basin (2.52 electron) and three disynaptic valence basins V(O₂,H₁), V(O₂,H₂), and V(O₂,C₂). One lone pair of this oxygen atom is forming a new dative bond with the H atom of the second CF₃OH molecule to create valence basin V(O₂,H₁). The simultaneous existence of V(O₂,H₁), V(O₂,H₂) with high populations of 1.68 and 1.73 electron, respectively, shows the strong attraction of oxygen for protons. The migrating fluorine F_m atom bears two valence basins V(C₁,H⁺F_m) and V(F_m,H₂) with average populations of 0.68 and 1.20 electron, respectively. The smaller V(C₁,F_m) population and the relatively higher V(F_m,H₂) populations show that the C₁-F_m bond is half broken and that F_m-H₂ bond formation is well advanced. Each H atom possesses a small monosynaptic basin corresponding to a small population (0.21–0.23 electron).

For **CF₃OH-2HFts**, the BCP network in Figure 10 is also consistent with simultaneous bond forming and breaking. Except for C, all heavy atoms are negatively charged, and the positive net charges of the migrating H-atoms are substantial. This confirms the simple model that in such cyclic reorganizations, the protons are transferred between the O/F lone pairs. Except for the CO bond, the forming/breaking bonds have a bond order of ~0.3, remarkably similar to those of **dim-6ts**.

Concluding Remarks

We have used high accuracy electronic structure methods to calculate a consistent set of basic thermochemical parameters, including the standard heats of formation, for trifluoromethanol and its derivatives. These calculated results are expected to have an accuracy of ±1.0 kcal/mol. From the calculated potential energy surfaces for elimination of hydrogen fluoride from trifluoromethanol in different reactant systems, we found that either a reactant CF₃OH or a product HF molecule present in the reaction medium can act as an acid–base bifunctional catalyst. However, these molecules exert the strongest catalytic effect within a trimeric system, involving either (HF)₂ or the (CF₃OH-HF) dimer in an eight-center chemical reaction. The H-transfer relay occurs within a compact and nearly planar eight-member cycle, and (HF)₂ appears to be a better autocatalyst. Although an energy barrier of ~20 kcal/mol with respect to the pre-association complex is present, the barrier with respect to reactants is only ~9 kcal/mol. The rate constants show that reactions 8 and 10–12 are all potential paths for CF₃OH decomposition with reaction 18 being the most likely. If we use the RRKM rate constant at 298 K, $k(298\text{ K}) = 1.76 \times 10^{-2}$

s^{-1} for reaction 11, we calculate the half-life for CF_3OH in the gas phase as less than 1 min when significant amounts of CF_3OH or HF are present at room temperature.

Acknowledgment. This work was supported in part by the Chemical Sciences, Geosciences and Biosciences Division, Office of Basic Energy Sciences, U.S. Department of Energy (DOE) under grant no. DE-FG02-03ER15481 (catalysis center program) and the National Science Foundation under Grant No. 0456343. D.A.D. is indebted to the Robert Ramsay Endowment of the University of Alabama. M.T.N. thanks the Flemish FWO-Vlaanderen for partly supporting his sabbatical leave at the University of Alabama.

Supporting Information Available: Total MP2 and CCSD-(T) energies (E_h) as a function of basis set extrapolated to the complete basis set limit. MP2 Vibrational modes (cm^{-1}). Skodje and Truhlar tunneling corrections (Q_{ST}). Rate constants with and without Q_{ST} . Symmetry and Cartesian coordinates of MP2/aVTZ optimized geometries. This material is available free of charge via the Internet at <http://pubs.acs.org>.

References and Notes

- (1) Seppelt, K. *Angew. Chem. Int. Ed.* **1977**, *16*, 322.
- (2) Kloeter, G.; Seppelt, K. *J. Am. Chem. Soc.* **1979**, *101*, 347.
- (3) Christe, K. O.; Hegge, J.; Hoge, B.; Haiges, R. *Angew. Chem., Int. Ed.* **2007**, *46*, 6155.
- (4) (a) Ravishankara, A. R.; Turnipseed, A. A.; Jensen, N. R.; Barone, S.; Mills, M.; Howard, C. J.; Solomon, S. *Science* **1994**, *263*, 71. (b) Ko, M. K. W. *Geophys. Res. Lett.* **1994**, *21*, 101.
- (5) Sehested, J.; Wallington, T. J. *Environ. Sci. Technol.* **1993**, *27*, 146.
- (6) Barone, S. R.; Turnipseed, A. A.; Ravishankara, A. R. *J. Phys. Chem.* **1994**, *98*, 4602.
- (7) (a) Lin, M. C. *J. Phys. Chem.* **1971**, *75*, 3642. (b) Lin, M. C. *J. Phys. Chem.* **1972**, *76*, 811.
- (8) Force, A. P.; Wiesenfeld, J. R. *J. Phys. Chem.* **1981**, *85*, 782.
- (9) Aker, D. M.; Niefer, B. I.; Sloan, J. J.; Heydtmann, H. *J. Chem. Phys.* **1987**, *87*, 203.
- (10) Clemmshaw, K. C.; Sodeau, J. R. *J. Phys. Chem.* **1989**, *93*, 3552.
- (11) (a) Francisco, J. S. *Chem. Phys.* **1991**, *150*, 19. (b) Francisco, J. S. *Chem. Phys. Lett.* **1994**, *218*, 401.
- (12) Schneider, W. F.; Wallington, T. J.; Huie, R. E. *J. Phys. Chem.* **1996**, *100*, 6097.
- (13) Huey, L. G.; Hanson, D. R.; Lovejoy, E. R. *J. Geophys. Res.* **1995**, *100*, 18771.
- (14) Lovejoy, E. R.; Huey, L. G.; Hanson, D. R. *J. Geophys. Res.* **1995**, *100*, 18775.
- (15) Komornicki, A.; Dixon, D. A.; Taylor, P. R. *J. Chem. Phys.* **1992**, *96*, 2920.
- (16) (a) Nguyen, M. T.; Ha, T. K. *J. Am. Chem. Soc.* **1984**, *106*, 599. (b) Nguyen, M. T.; Hegarty, A. F. *J. Am. Chem. Soc.* **1983**, *105*, 3811.
- (17) (a) Parra, R. D.; Zeng, X. C. *J. Chem. Phys.* **1999**, *110*, 6329. (b) Doering, W. E.; Parra, R. D.; Zeng, X. C. *J. Chem. Phys.* **1998**, *431*, 119.
- (18) Bock, C. W.; Trachman, M.; Niki, H.; Mains, G. J. *J. Phys. Chem.* **1995**, *99*, 4354.
- (19) Ruelle, P. *J. Am. Chem. Soc.* **1987**, *109*, 1722.
- (20) Benson, S. W. *J. Phys. Chem.* **1994**, *98*, 2216.
- (21) Schneider, W. F.; Wallington, T. J.; Hurley, M. D.; Sehested, J.; Nielsen, O. J. *J. Phys. Chem.* **1994**, *98*, 2217.
- (22) Schneider, W. F.; Wallington, T. J. *J. Phys. Chem.* **1995**, *99*, 4353.
- (23) (a) Batt, L.; Walsh, R. *Int. J. Chem. Kinet.* **1982**, *14*, 933. (b) Batt, L.; Walsh, R. *Int. J. Chem. Kinet.* **1983**, *15*, 605.
- (24) Wallington, T. J.; Hurley, M. D.; Sehested, J.; Nielsen, O. J. *J. Phys. Chem.* **1993**, *97*, 7606.
- (25) Sana, M.; Leroy, G.; Peeters, D.; Wilante, C. *J. Mol. Struct. (THEOCHEM)* **1988**, *164*, 249.
- (26) Dixon, D. A.; Fernandez, R. Proceedings of the STEP-HALOCSIDE AFEAS Workshop, Dublin, Ireland, March 1993.
- (27) (a) Schneider, W. F.; Wallington, T. J. *J. Phys. Chem.* **1993**, *97*, 12783. (b) Schneider, W. F.; Wallington, T. J. *J. Phys. Chem.* **1994**, *98*, 7448. (c) Schneider, W. F.; Nance, B. I.; Wallington, T. J. *J. Am. Chem. Soc.* **1995**, *117*, 478.
- (28) Bock, C. W.; Trachman, M.; Niki, H.; Mains, G. J. *J. Phys. Chem.* **1994**, *98*, 7976.
- (29) Montgomery, J. A.; Michels, H. H.; Francisco, J. S. *Chem. Phys. Lett.* **1994**, *220*, 391.
- (30) Chyall, L. J.; Squires, R. R. *J. Phys. Chem.* **1996**, *100*, 16435.
- (31) Asher, R. L.; Appelman, E. H.; Tilson, J. L.; Litorja, M.; Berkovitz, J.; Ruscic, B. *J. Chem. Phys.* **1997**, *106*, 9111.
- (32) Reints, W.; Pratt, D. A.; Korth, H. G.; Mulder, P. *J. Phys. Chem. A* **2000**, *104*, 10713.
- (33) Huey, L. G.; Dunlea, E. J.; Howard, C. J. *J. Phys. Chem.* **1996**, *100*, 6504.
- (34) Notario, R.; Castano, O.; Abboud, J. L. M. *Chem. Phys. Lett.* **1996**, *263*, 367.
- (35) (a) Francisco, J. S.; Li, Z.; Williams, I. H. *Chem. Phys. Lett.* **1991**, *186*, 343. (b) Li, Z.; Francisco, J. S. *Chem. Phys. Lett.* **1991**, *186*, 336.
- (36) Cui, Q.; Morokuma, K. *Chem. Phys. Lett.* **1996**, *263*, 54.
- (37) Barckholtz, T. A.; Miller, T. A. *J. Phys. Chem. A* **1999**, *103*, 2321.
- (38) Arguello, G. A.; Willner, H. *J. Phys. Chem. A* **2001**, *105*, 3466.
- (39) Larson, J. W.; McMahon, T. B. *J. Am. Chem. Soc.* **1983**, *105*, 2944.
- (40) Spyrou, S. M.; Hunter, S. R.; Christophorou, L. G. *J. Chem. Phys.* **1984**, *81*, 4481.
- (41) Taft, R. W.; Koppel, I. J.; Topsom, R. D.; Anvia, F. *J. Am. Chem. Soc.* **1990**, *112*, 2047.
- (42) Morris, R. A.; Miller, T. M.; Paulson, J. F.; Viggiano, A. A.; Feldmann, M. T.; King, R. A.; Schaefer, H. F. *J. Chem. Phys.* **1999**, *110*, 8436.
- (43) (a) Feller, D.; Peterson, K. A. *J. Chem. Phys.* **1998**, *108*, 154. (b) Feller, D.; Peterson, K. A. *J. Chem. Phys.* **1999**, *110*, 8384. (c) Feller, D.; Dixon, D. A. *J. Phys. Chem. A* **1999**, *103*, 6413. (d) Feller, D. *J. Chem. Phys.* **1999**, *111*, 4373. (e) Feller, D.; Dixon, D. A. *J. Phys. Chem. A* **2000**, *104*, 3048. (f) Feller, D.; Sordo, J. A. *J. Chem. Phys.* **2000**, *113*, 485. (g) Feller, D.; Franz, J. A. *J. Phys. Chem. A* **2000**, *104*, 9017. (h) Feller, D.; Dixon, D. A. *J. Chem. Phys.* **2001**, *115*, 3484. (i) Dixon, D. A.; Feller, D.; Sandrone, G. *J. Phys. Chem. A* **1999**, *103*, 4744. (j) Ruscic, B.; Feller, D.; Dixon, D. A.; Peterson, K. A.; Harding, L. B.; Asher, R. L.; Wagner, A. F. *J. Phys. Chem. A* **2001**, *105*, 1. (k) Ruscic, B.; Wagner, A. F.; Harding, L. B.; Asher, R. L.; Feller, D.; Dixon, D. A.; Peterson, K. A.; Song, Y.; Qian, X.; Ng, C.; Liu, J.; Chen, W.; Schwenke, D. W. *J. Phys. Chem. A* **2002**, *106*, 2727.
- (44) Matus, M. H.; Nguyen, M. T.; Dixon, D. A. *J. Phys. Chem. A* **2007**, *111*, 113.
- (45) Frisch, M. J.; Trucks, G. W.; Schlegel, H. B.; Scuseria, G. E.; Robb, M. A.; Cheeseman, J. R.; Montgomery, J. A., Jr.; Vreven, T.; Kudin, K. N.; Burant, J. C.; Millam, J. M.; Iyengar, S. S.; Tomasi, J.; Barone, V.; Mennucci, B.; Cossi, M.; Scalmani, G.; Rega, N.; Petersson, G. A.; Nakatsuji, H.; Hada, M.; Ehara, M.; Toyota, K.; Fukuda, R.; Hasegawa, J.; Ishida, M.; Nakajima, T.; Honda, Y.; Kitao, O.; Nakai, H.; Klene, M.; Li, X.; Knox, J. E.; Hratchian, H. P.; Cross, J. B.; Bakken, V.; Adamo, C.; Jaramillo, J.; Gomperts, R.; Stratmann, R. E.; Yazyev, O.; Austin, A. J.; Cammi, R.; Pomelli, C.; Ochterski, J. W.; Ayala, P. Y.; Morokuma, K.; Voth, G. A.; Salvador, P.; Dannenberg, J. J.; Zakrzewski, V. G.; Dapprich, S.; Daniels, A. D.; Strain, M. C.; Farkas, O.; Malick, D. K.; Rabuck, A. D.; Raghavachari, K.; Foresman, J. B.; Ortiz, J. V.; Cui, Q.; Baboul, A. G.; Clifford, S.; Cioslowski, J.; Stefanov, B. B.; Liu, G.; Liashenko, A.; Piskorz, P.; Komaromi, I.; Martin, R. L.; Fox, D. J.; Keith, T.; Al-Laham, M. A.; Peng, C. Y.; Nanayakkara, A.; Challacombe, M.; Gill, P. M. W.; Johnson, B.; Chen, W.; Wong, M. W.; Gonzalez, C.; Pople, J. A. *Gaussian 03*, revision C.01; Gaussian, Inc.: Wallingford, CT, 2004.
- (46) Werner, H.-J.; Knowles, P. J.; Lindh, R.; Manby, F. R.; Schütz, M.; Celani, P.; Korona, T.; Rauhut, G.; Amos, R. D.; Bernhardsson, A.; Berning, A.; Cooper, D. L.; Deegan, M. J. O.; Dobbyn, A. J.; Eckert, F.; Hampel, C.; Hetzer, G.; Lloyd, A. W.; McNicholas, S. J.; Meyer, W.; Mura, M. E.; Nicklass, A.; Palmieri, P.; Pitzer, R.; Schumann, U.; Stoll, H.; Stone, A. J.; Tarroni, R.; Thorsteinsson, T. MOLPRO, version 2006.1, a package of ab initio programs; Universität Stuttgart, Stuttgart, Germany, and University of Cardiff, Cardiff, Wales, United Kingdom. See <http://www.molpro>.
- (47) Purvis, G. D., III; Bartlett, R. J. *J. Chem. Phys.* **1982**, *76*, 1910.
- (48) Raghavachari, K.; Trucks, G. W.; Pople, J. A.; Head-Gordon, M. *Chem. Phys. Lett.* **1989**, *157*, 479.
- (49) Watts, J. D.; Gauss, J.; Bartlett, R. J. *J. Chem. Phys.* **1993**, *98*, 8718.
- (50) Bartlett, R. J.; Musial, M. *Rev. Mod. Phys.* **2007**, *79*, 291.
- (51) (a) Dunning, T. H. *J. Chem. Phys.* **1989**, *90*, 1007. (b) Kendall, R. A.; Dunning, T. H.; Harrison, R. J. *J. Chem. Phys.* **1992**, *96*, 6796.
- (52) Rittby, M.; Bartlett, R. J. *J. Phys. Chem.* **1988**, *92*, 3033.
- (53) Knowles, P. J.; Hampel, C.; Werner, H.-J. *J. Chem. Phys.* **1994**, *99*, 5219.
- (54) Deegan, M. J. O.; Knowles, P. J. *Chem. Phys. Lett.* **1994**, *227*, 321.
- (55) Peterson, K. A.; Woon, D. E.; Dunning, T. H., Jr. *J. Chem. Phys.* **1994**, *100*, 7410.
- (56) Serallach, A.; Meyer, R.; Günthard, H. H. *J. Mol. Spectrosc.* **1974**, *52*, 94.

- (57) Fernández, L. E.; Varetti, E. L. *J. Mol. Struct. (THEOCHEM)* **2003**, 629, 175.
- (58) Shimanouchi, T. *Tables of Molecular Vibrational Frequencies; Consolidated Volume 1*, NSRDS NBS-39; U.S. Department of Commerce, National Technical Information Service: Washington, D.C., 1972.
- (59) Serallach, A.; Meyer, R.; Günthard, H. H. *J. Mol. Spectrosc.* **1974**, 84, 94.
- (60) (a) Helgaker, T.; Klopper, W.; Koch, H.; Nagel, J. J. *Chem. Phys.* **1997**, 106, 9639. (b) Halkier, A.; Helgaker, T.; Jørgensen, P.; Klopper, W.; Koch, H.; Olsen, J.; Wilson, A. K. *Chem. Phys. Lett.* **1998**, 286, 243.
- (61) Davidson, E. R.; Ishikawa, Y.; Malli, G. L. *Chem. Phys. Lett.* **1981**, 84, 226.
- (62) Moore, C. E. *Atomic energy levels as derived from the analysis of optical spectra, Volume 1, H to V*; U.S. National Bureau of Standards Circular 467; U.S. Department of Commerce, National Technical Information Service, COM-72-50282; Washington, D.C., 1949.
- (63) Chase, M. W., Jr. NIST-JANAF Tables, 4th ed. *J. Phys. Chem. Ref. Data* **1998**, Mono. 9, Suppl. 1..
- (64) Curtiss, L. A.; Raghavachari, K.; Redfern, P. C.; Pople, J. A. *J. Chem. Phys.* **1997**, 106, 1063.
- (65) Steinfeld, J. I.; Francisco, J. S.; Hase, W. L. *Chemical Kinetics and Dynamics*, 2nd ed.; Prentice Hall: Englewood Cliffs, NJ, 1999.
- (66) (a) Kreevoy, M. M.; Truhlar, D. G. In *Transition State Theory in Investigations of Rates and Mechanisms of Reactions*, 4th ed.; Bernasconi, C. F., Ed.; Wiley: New York, 1986. (b) Johnston, H. S. *Gas Phase Reaction Rate Theory*; Ronald Press: New York, 1966. (c) Glasstone, S.; Laidler, K. J.; Eyring, H. *The Theory of Rate Processes*; McGraw-Hill: New York, 1941. (d) Garrett, B. C.; Truhlar, D. G. *Transition State Theory*. In *Encyclopedia of Computational Chemistry*; Schleyer, P. v. R., Allinger, N. L., Clark, T., Gasteiger, J., Kollman, P. A., Schaefer, H. F., III, Eds.; John Wiley & Sons: Chichester, U.K., 1998.
- (67) Holbrook, K. A.; Pilling, M. J.; Robertson, S. H. *Unimolecular Reactions*, 2nd ed.; Wiley: Chichester, U.K., 1996.
- (68) KHIMERA, Version 3.2: A software tool for calculations of chemical reactions thermodynamics and kinetics from first principles, Kintech, Kinetic Technologies, Ltd., Moscow, 2003; <http://www.kintech.ru/>.
- (69) Skodje, R. T.; Truhlar, D. J. *J. Chem. Phys.* **1981**, 85, 624.
- (70) Sander, S. P.; Friedl, R. R.; Ravishankara, A. R.; Golden, D. M.; Kolb, C. E.; Kurylo, M. J.; Huie, R. E.; Orkin, V. L.; Molina, M. J.; Moortgat, G. K.; Finlayson-Pitts, B. J. *Chemical Kinetics and Photochemical Data for Use in Atmospheric Studies: Evaluation Number 14*; JPL Publication 02-25; National Aeronautics and Space Administration, Jet Propulsion Laboratory, California Institute of Technology: Pasadena, CA, 2003; http://jpldataeval.jpl.nasa.gov/pdf/JPL_02-25_rev02.pdf.
- (71) Grandinetti, F.; Occhiucci, G.; Crestoni, M. E.; Forarini, S.; Speranza, M. *Int. J. Mass Spectrom. Ion Processes* **1993**, 127, 123.
- (72) (a) Doiron, C. E.; McMahon, T. B. *Can. J. Chem.* **1984**, 59, 2689. (b) Collyer, S. M.; McMahon, T. B. *J. Phys. Chem.* **1983**, 87, 909.
- (73) (a) Marenich, A. V.; Boggs, J. E. *J. Phys. Chem. A* **2007**, 111, 11214. (b) Marenich, A. V.; Boggs, J. E. *Int. J. Quant. Chem.* **2006**, 106, 2609, and references therein.
- (74) Farnham, W. B.; Smart, B. E.; Middleton, W. J.; Calabrese, J. C.; Dixon, D. A. *J. Am. Chem. Soc.* **1985**, 107, 4565.
- (75) Krespan, C. G.; Dixon, D. A. *J. Fluorine Chem.* **1996**, 77, 117.
- (76) Christe, K. O.; Dixon, D. A.; McLemore, D. K.; Wilson, W. W.; Sheehy, J.; Boatz, J. A. *J. Fluorine Chem.* **2000**, 101, 151.
- (77) NIST Database, <http://webbook.nist.gov>.
- (78) Segovia, M.; Ventura, O. N. *Chem. Phys. Lett.* **1997**, 277, 490.
- (79) Asher, R. L.; Appelman, E. H.; Ruscic, B. *J. Chem. Phys.* **1996**, 105, 9781.
- (80) Dixon, D. A.; Feller, D. *J. Phys. Chem. A* **1998**, 102, 8209.
- (81) Srinivasan, N. K.; Su, M.-C.; Michael, J. V.; Klippenstein, S. J.; Harding, L. B. *J. Phys. Chem. A* **2007**, 111, 6822.
- (82) Liedl, K. R.; Sesušak, S.; Kroemer, R. T.; Rode, B. M. *J. Phys. Chem. A* **1997**, 101, 4707.
- (83) (a) Bader, R. F. W. *Atoms in Molecules, A Quantum Theory*, Oxford University Press, 1995. (b) Popelier, P. *Atoms in Molecules. An Introduction*; Prentice Hall: Englewood Cliffs, NJ, 2000.
- (84) (a) Becke, A. D.; Edgecombe, K. E. *J. Chem. Phys.* **1990**, 92, 5397. (b) Silvi, B.; Savin, A. *Nature* **1994**, 371, 63.
- (85) Nguyen, M. T.; Nguyen, V. S.; Matus, M. H.; Gopakumar, G.; Dixon, D. A. *J. Phys. Chem. A* **2007**, 111, 679.